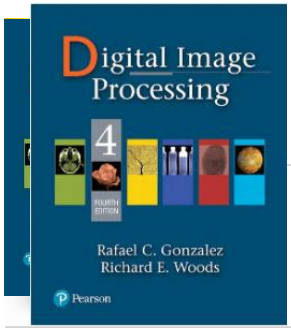

Chapter 4
Filtering in the Frequency Domain

Filtering in the Frequency Domain (II)

Dr. Tun-Wen Pai

1) **LP/HP/BP/BS filters in frequency domain**
2) **Ideal filtering effects**
3) **Homomorphic filter**

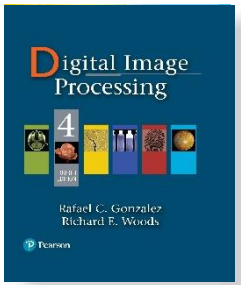

Digital Image Processing, 4th ed.

Gonzalez & Woods

www.ImageProcessingPlace.com

Chapter 4
Filtering in the Frequency Domain

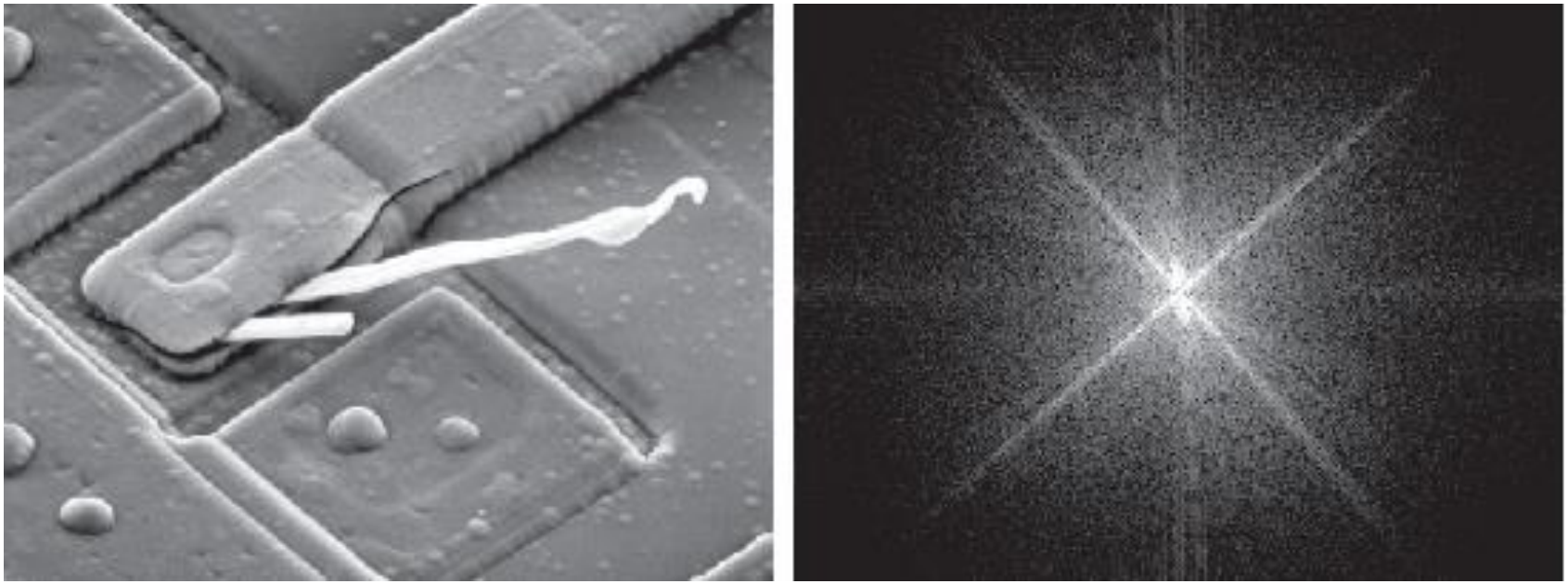

a b

FIGURE 4.28 (a) SEM image of a damaged integrated circuit. (b) Fourier spectrum of (a). (Original image courtesy of Dr. J. M. Hudak, Brockhouse Institute for Materials Research, McMaster University, Hamilton, Ontario, Canada.)

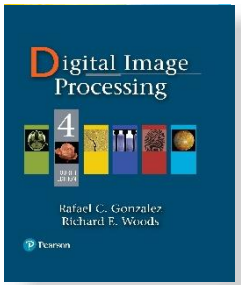

Chapter 4
Filtering in the Frequency Domain

FIGURE 4.29
Result of filtering the image in Fig. 4.28(a) with a filter transfer function that sets to 0 the dc term, $F(P/2, Q/2)$, in the centered Fourier transform, while leaving all other transform terms unchanged.

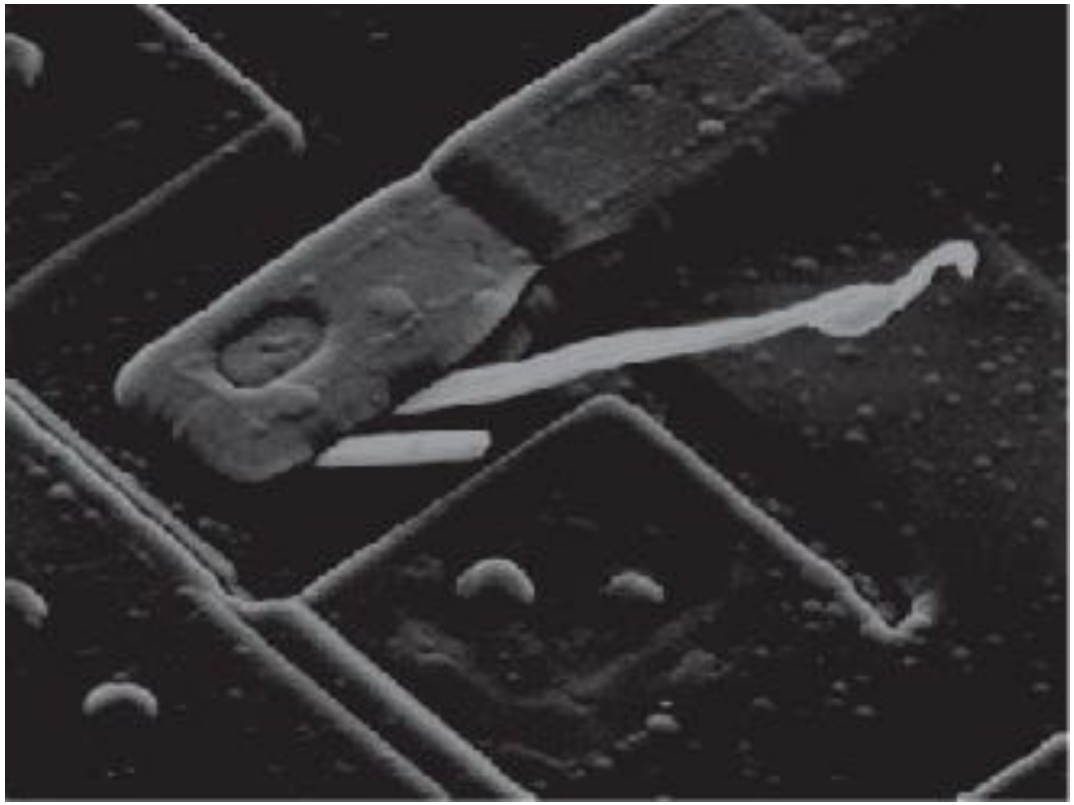

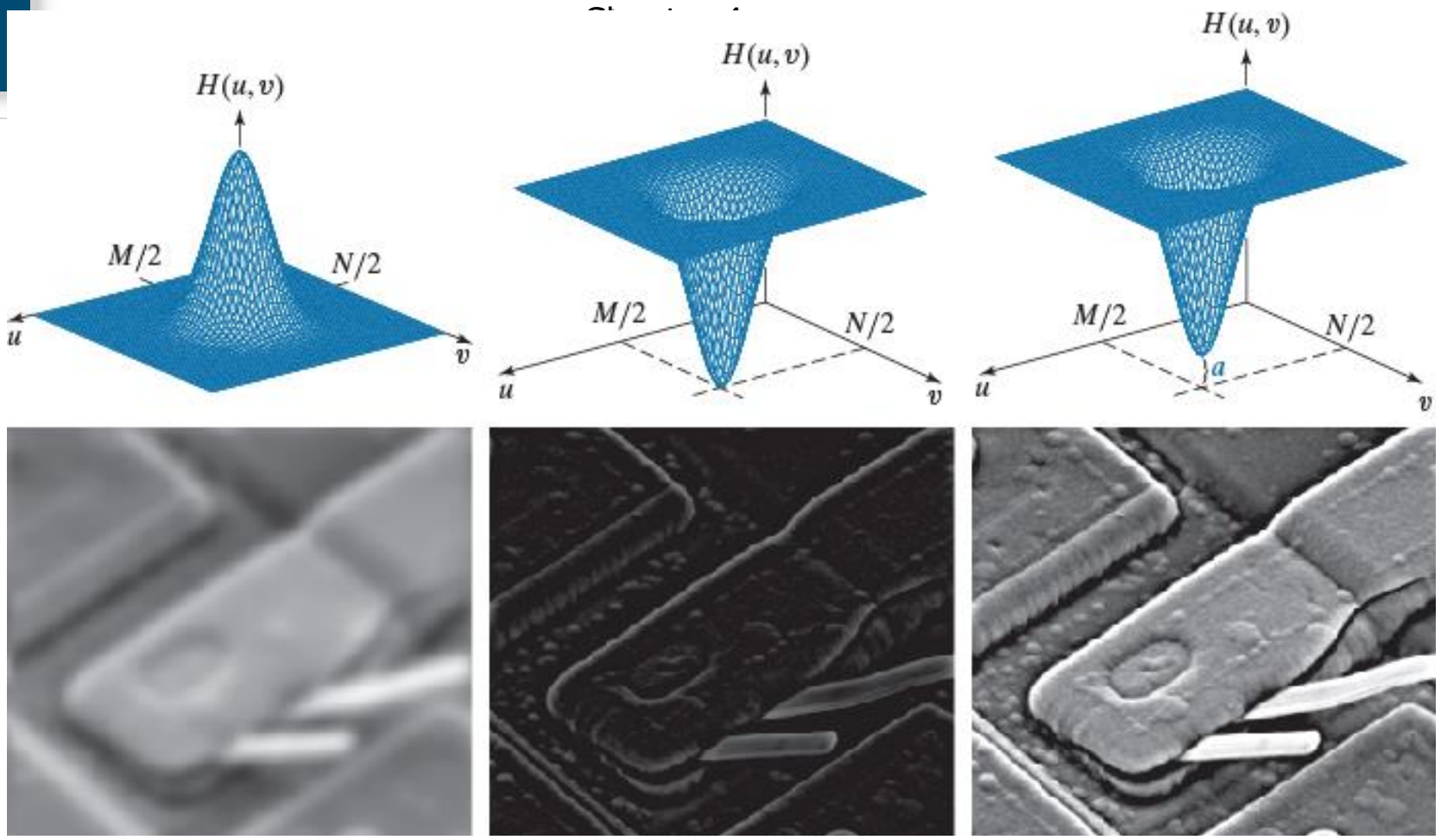

a b c
d e f

FIGURE 4.30 Top row: Frequency domain filter transfer functions of (a) a lowpass filter, (b) a highpass filter, and (c) an offset highpass filter. Bottom row: Corresponding filtered images obtained using Eq. (4-104). The offset in (c) is $a = 0.85$, and the height of $H(u,v)$ is 1. Compare (f) with Fig. 4.28(a).

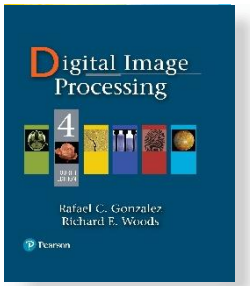

Digital Image Processing, 4th ed.

Gonzalez & Woods

Chapter 4
Filtering in the Frequency Domain

a b c

FIGURE 4.31 (a) A simple image. (b) Result of blurring with a Gaussian lowpass filter without padding. (c) Result of lowpass filtering with zero padding. Compare the vertical edges in (b) and (c).

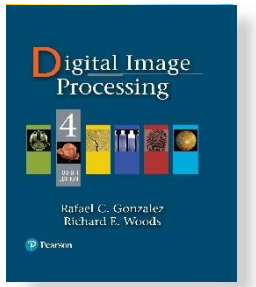

Chapter 4
Filtering in the Frequency Domain

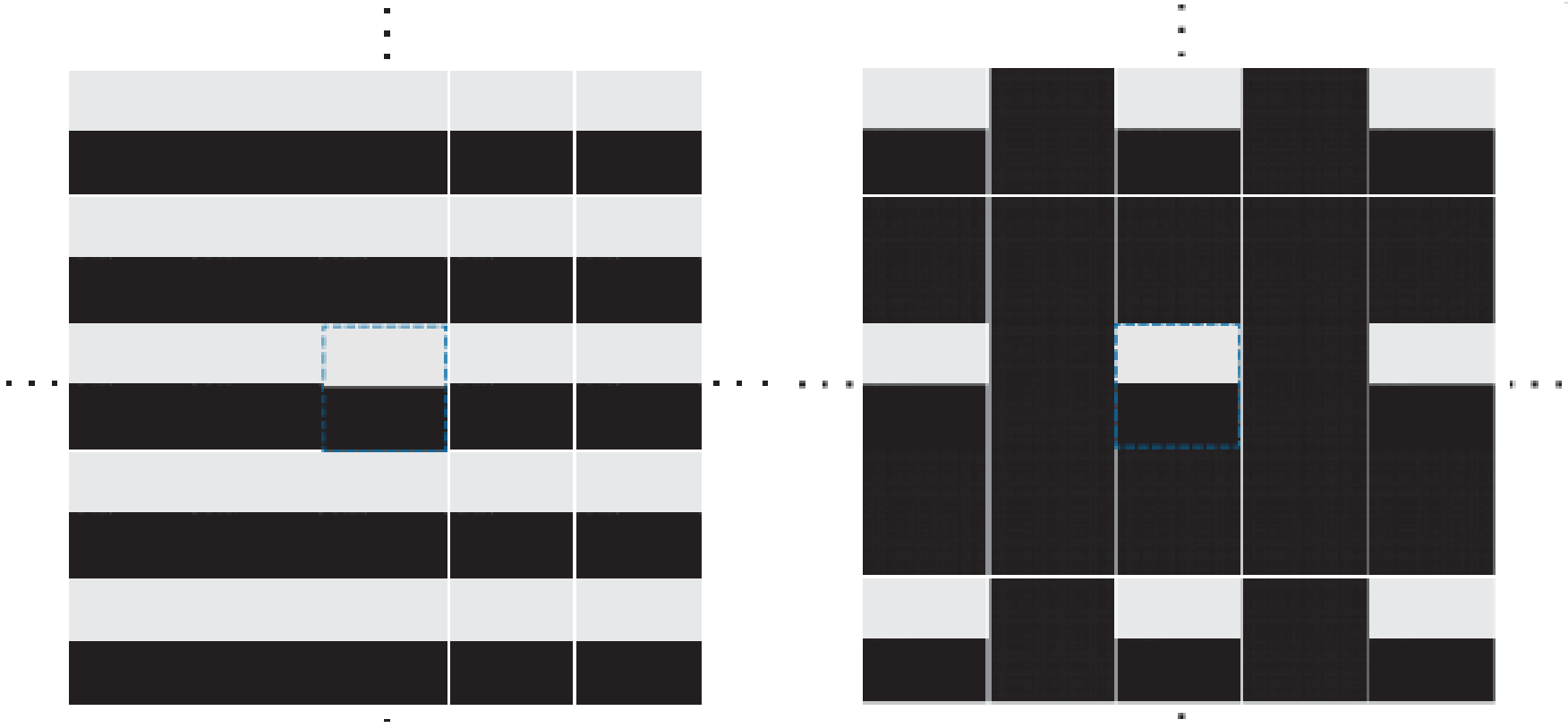

a b

FIGURE 4.32 (a) Image periodicity without image padding. (b) Periodicity after padding with 0's (black). The dashed areas in the center correspond to the image in Fig. 4.31(a). Periodicity is inherent when using the DFT. (The thin white lines in both images are superimposed for clarity; they are not part of the data.)

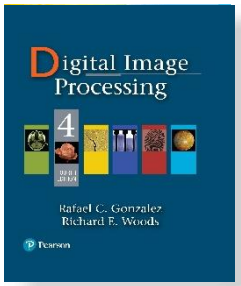

Chapter 4
Filtering in the Frequency Domain

a c
b d

FIGURE 4.33
(a) Filter transfer function specified in the (centered) frequency domain. (b) Spatial representation (filter kernel) obtained by computing the IDFT of (a). (c) Result of padding (b) to twice its length (note the discontinuities). (d) Corresponding filter in the frequency domain obtained by computing the DFT of (c). Note the ringing caused by the discontinuities in (c). Part (b) of the figure is below (a), and (d) is below (c).

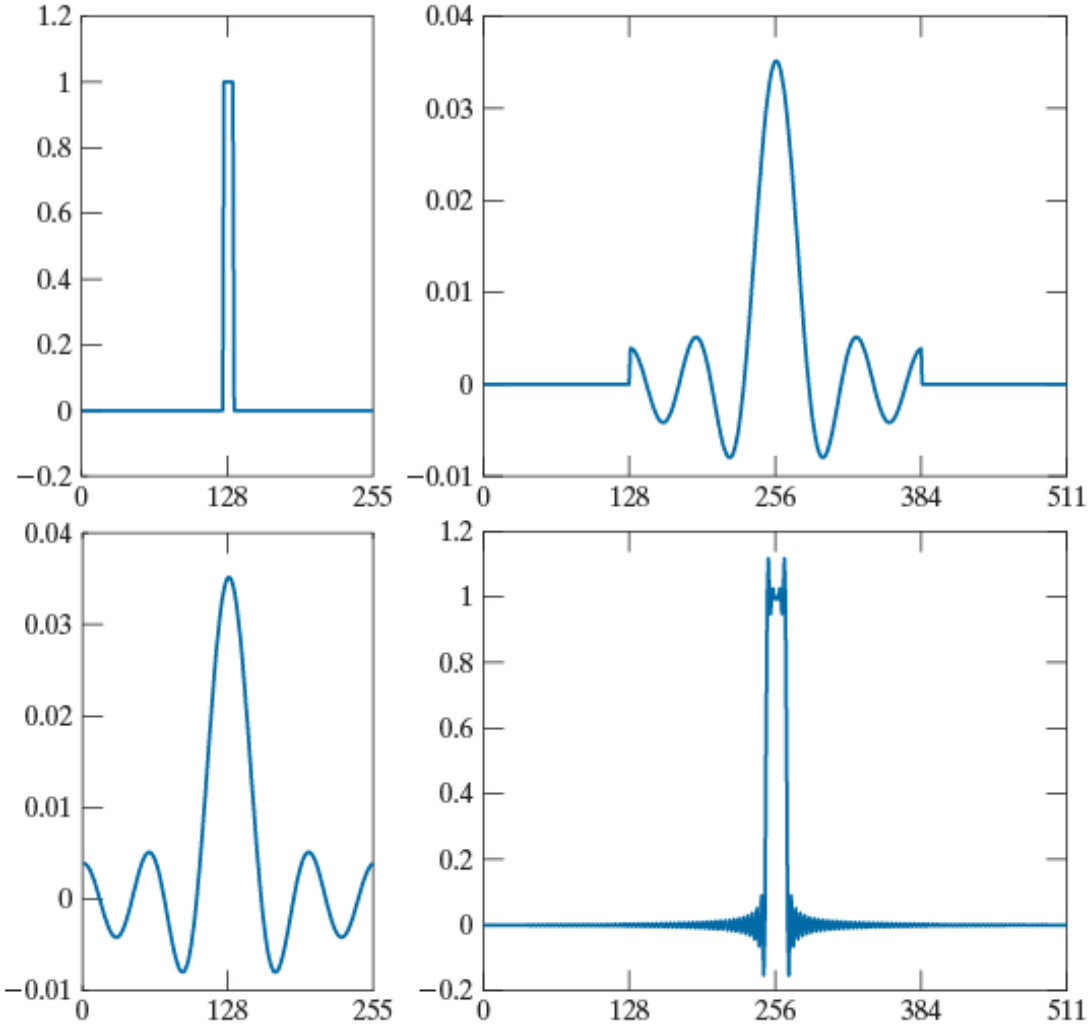

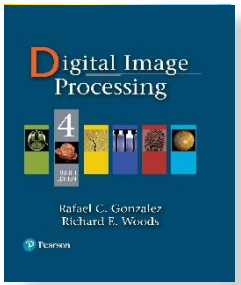

Chapter 4
Filtering in the Frequency Domain

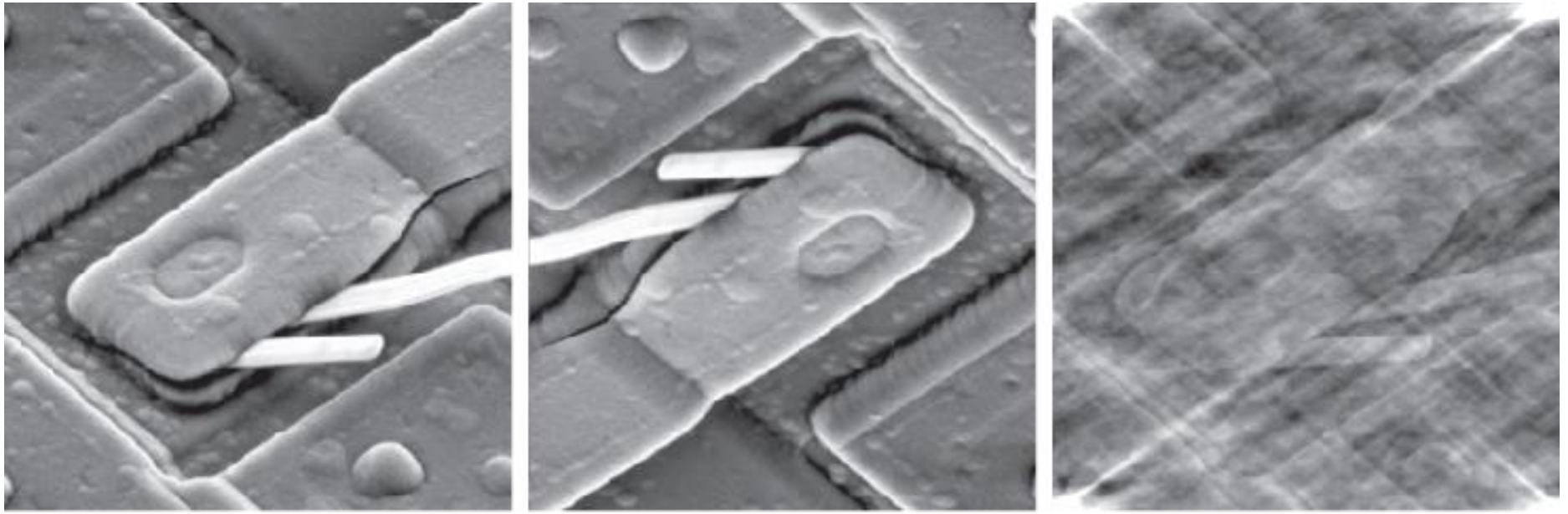

a b c

FIGURE 4.34 (a) Original image. (b) Image obtained by multiplying the phase angle array by −1 in Eq. (4-86) and computing the IDFT. (c) Result of multiplying the phase angle by 0.25 and computing the IDFT. The magnitude of the transform, $|F(u,v)|$, used in (b) and (c) was the same.

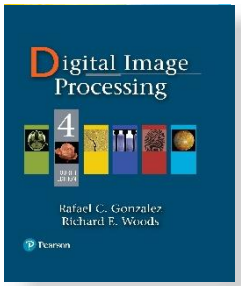

Chapter 4
Filtering in the Frequency Domain

a b c
d e f
g h

FIGURE 4.35
(a) An $M \times N$ image, f.
(b) Padded image, f_p of size $P \times Q$.
(c) Result of multiplying f_p by $(-1)^{x+y}$.
(d) Spectrum of F. (e) Centered Gaussian lowpass filter transfer function, H, of size $P \times Q$.
(f) Spectrum of the product HF.
(g) Image g_p, the real part of the IDFT of HF, multiplied by $(-1)^{x+y}$.
(h) Final result, g, obtained by extracting the first M rows and N columns of g_p.

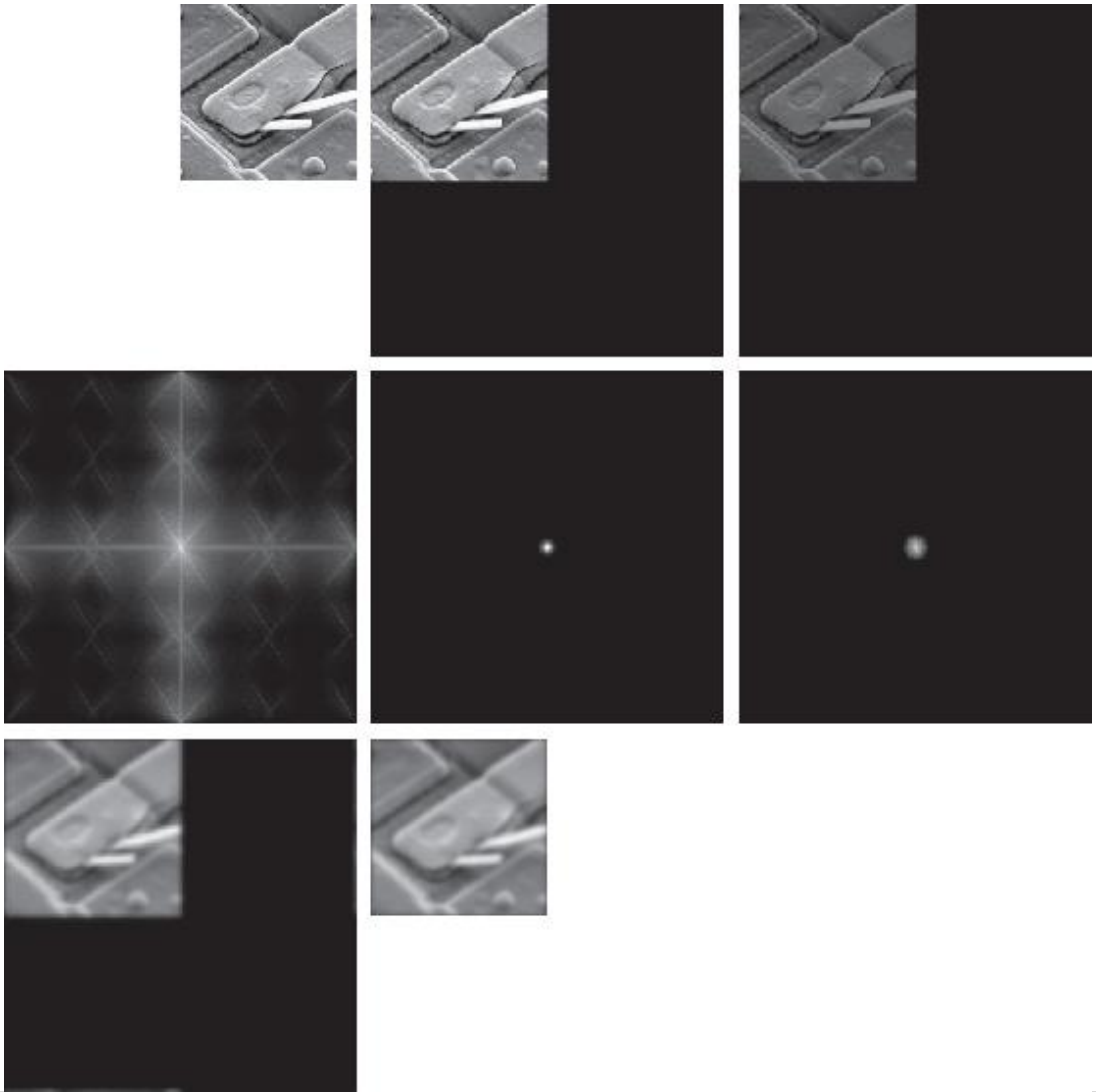

Chapter 4
Filtering in the Frequency Domain

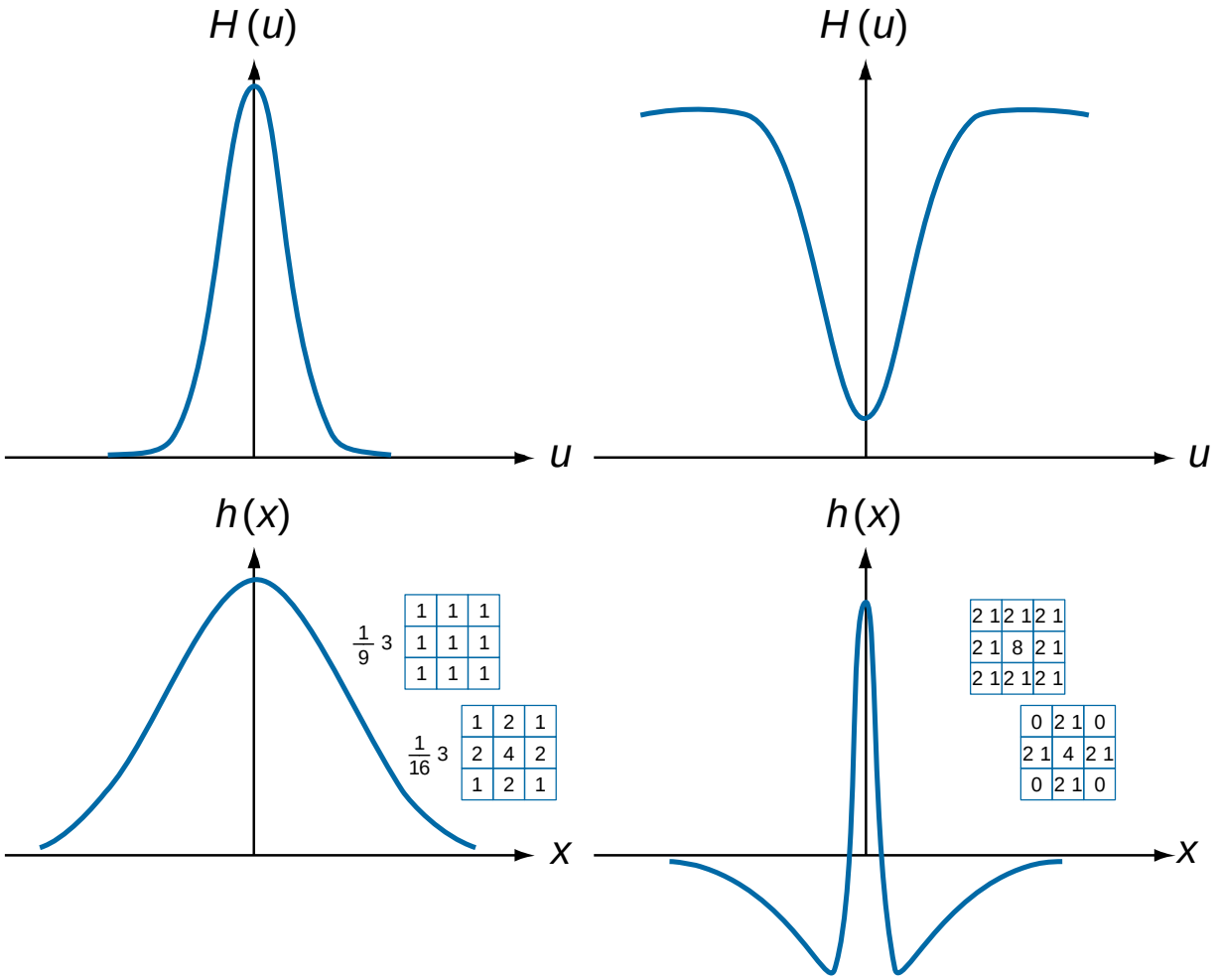

a c
b d

FIGURE 4.36
(a) A 1-D Gaussian lowpass transfer function in the frequency domain. (b) Corresponding kernel in the spatial domain. (c) Gaussian highpass transfer function in the frequency domain. (d) Corresponding kernel. The small 2-D kernels shown are kernels we used in Chapter 3.

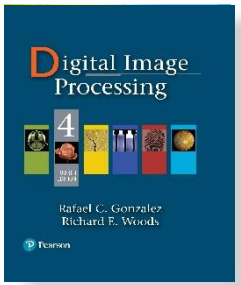

Chapter 4
Filtering in the Frequency Domain

a b

FIGURE 4.37
(a) Image of a building, and (b) its Fourier spectrum.

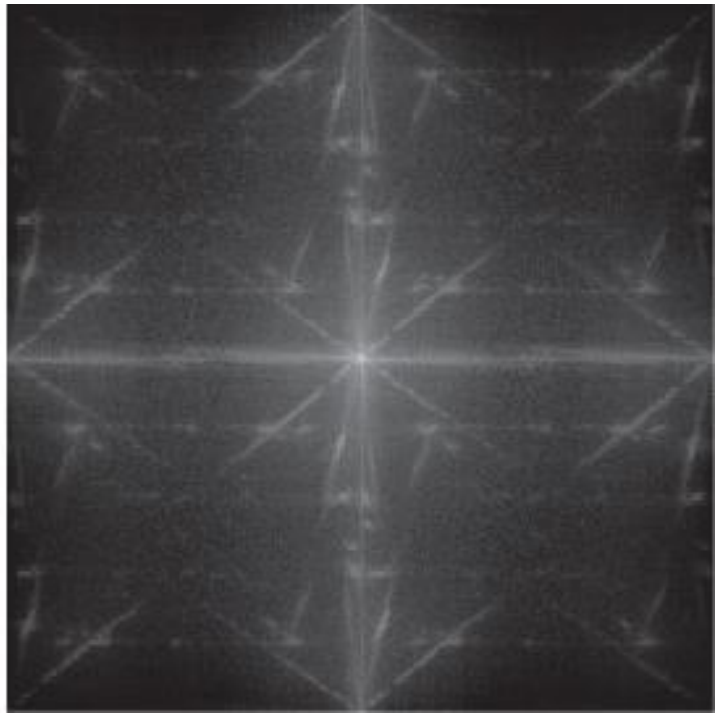

Chapter 4
Filtering in the Frequency Domain

a b
c d

FIGURE 4.38
(a) A spatial kernel and perspective plot of its corresponding frequency domain filter transfer function.
(b) Transfer function shown as an image.
(c) Result of filtering Fig. 4.37(a) in the frequency domain with the transfer function in (b).
(d) Result of filtering the same image in the spatial domain with the kernel in (a). The results are identical.

−1	0	1
−2	0	2
−1	0	1

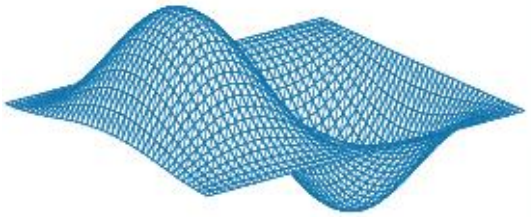

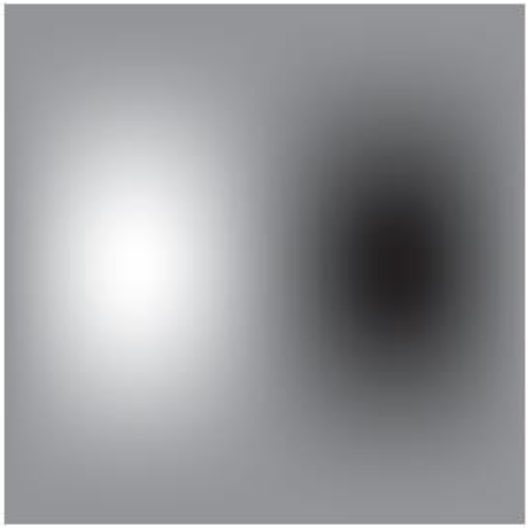

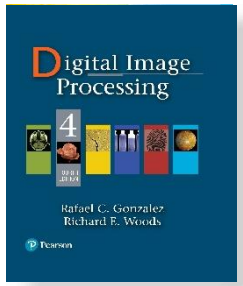

Chapter 4
Filtering in the Frequency Domain

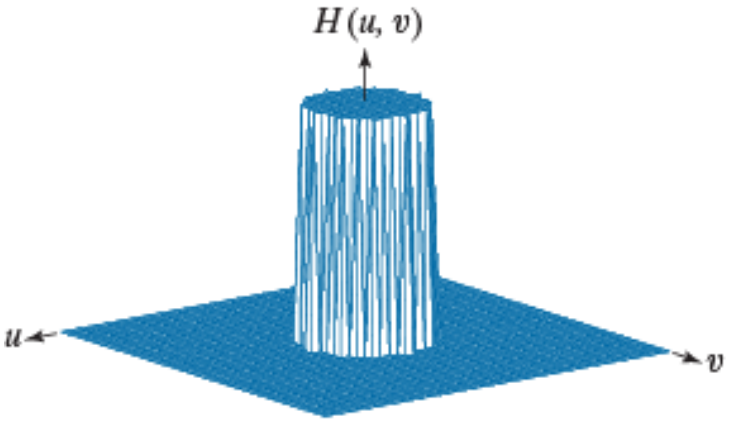

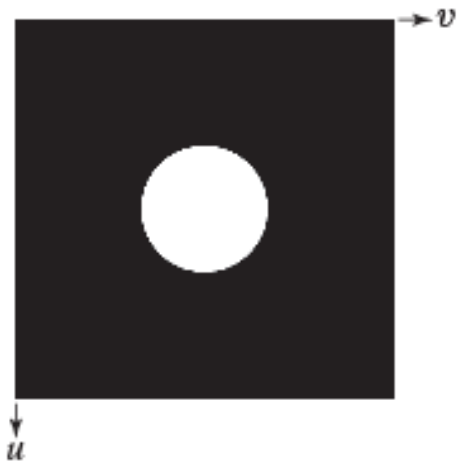

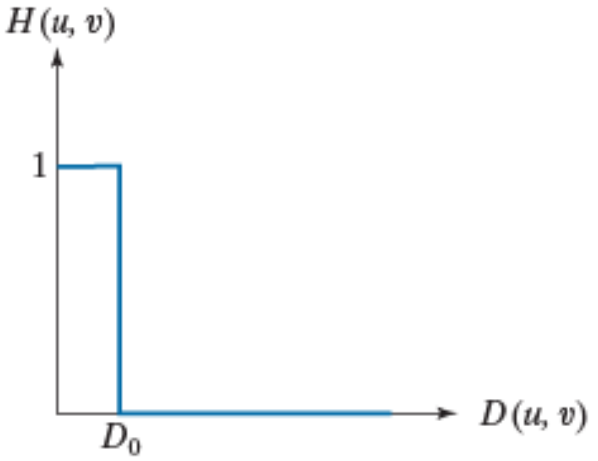

a b c

FIGURE 4.39 (a) Perspective plot of an ideal lowpass-filter transfer function. (b) Function displayed as an image. (c) Radial cross section.

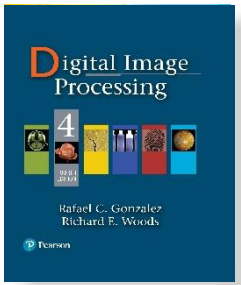

Chapter 4
Filtering in the Frequency Domain

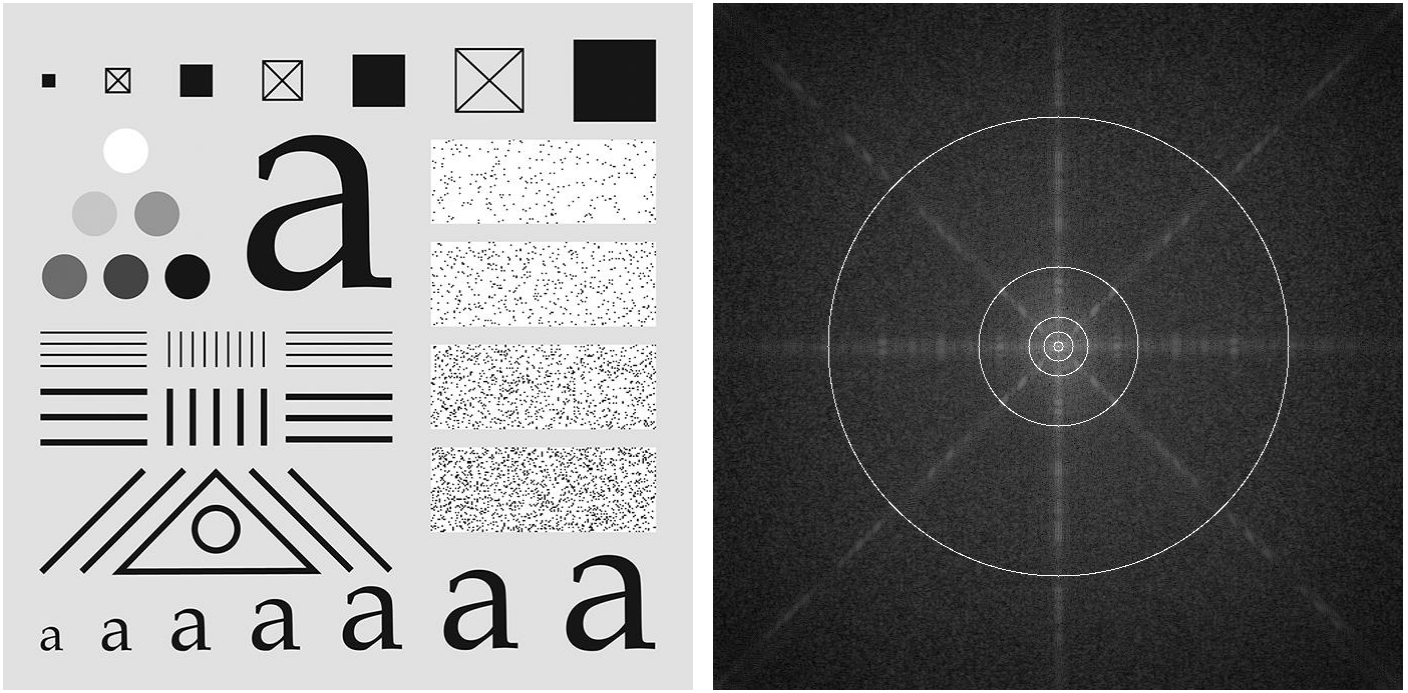

a b

FIGURE 4.40 (a) Test pattern of size 688 × 688 pixels, and (b) its spectrum. The spectrum is double the image size as a result of padding, but is shown half size to fit. The circles have radii of 10, 30, 60, 160, and 460 pixels with respect to the full-size spectrum. The radii enclose 86.9, 92.8, 95.1, 97.6, and 99.4% of the padded image power, respectively.

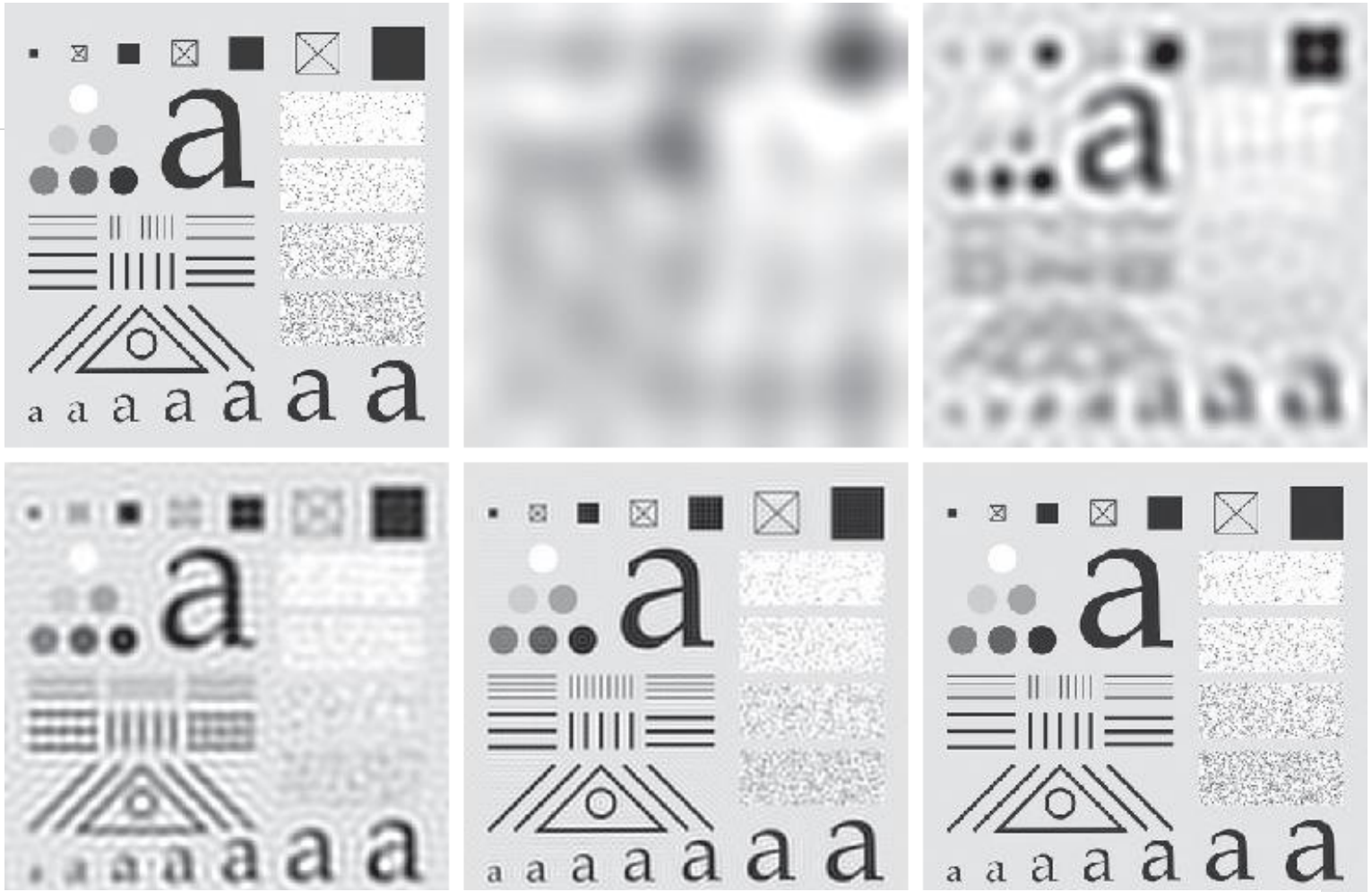

a b c
d e f

FIGURE 4.41 (a) Original image of size 688 × 688 pixels. (b)–(f) Results of filtering using ILPFs with cutoff frequencies set at radii values 10, 30, 60, 160, and 460, as shown in Fig. 4.40(b). The power removed by these filters was 13.1, 7.2, 4.9, 2.4, and 0.6% of the total, respectively. We used mirror padding to avoid the black borders characteristic of zero padding, as illustrated in Fig. 4.31(c).

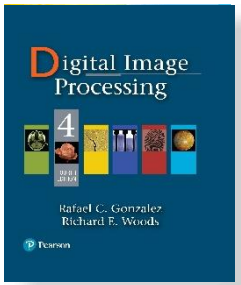

Chapter 4
Filtering in the Frequency Domain

a b c

FIGURE 4.42
(a) Frequency domain ILPF transfer function. (b) Corresponding spatial domain kernel function. (c) Intensity profile of a horizontal line through the center of (b).

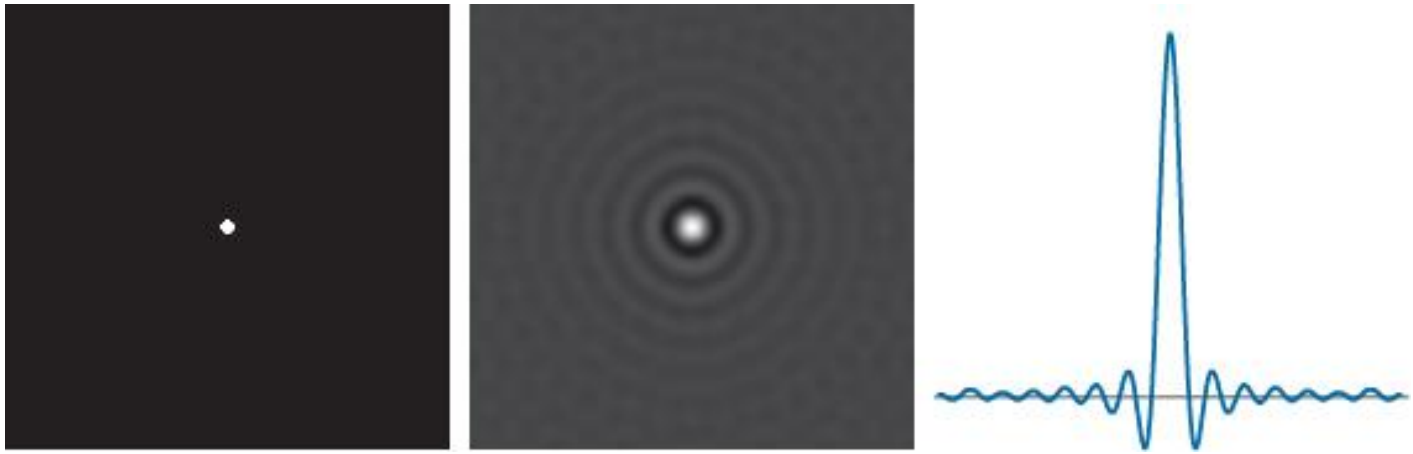

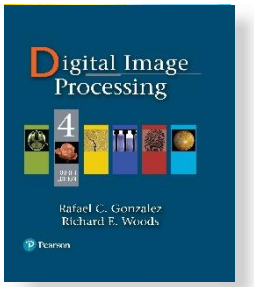

Chapter 4
Filtering in the Frequency Domain

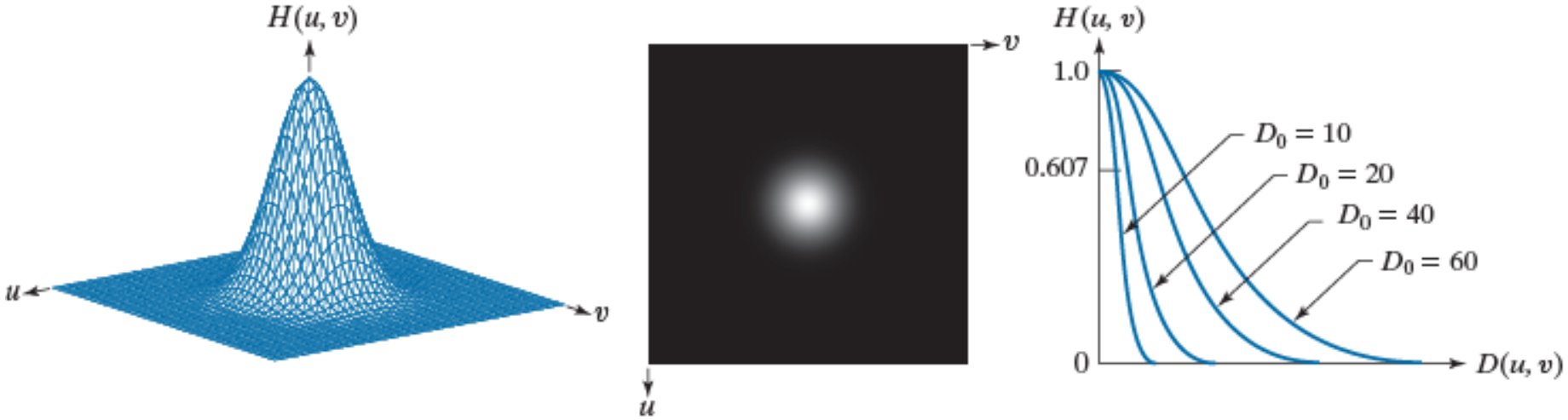

a b c

FIGURE 4.43 (a) Perspective plot of a GLPF transfer function. (b) Function displayed as an image. (c) Radial cross sections for various values of D_0.

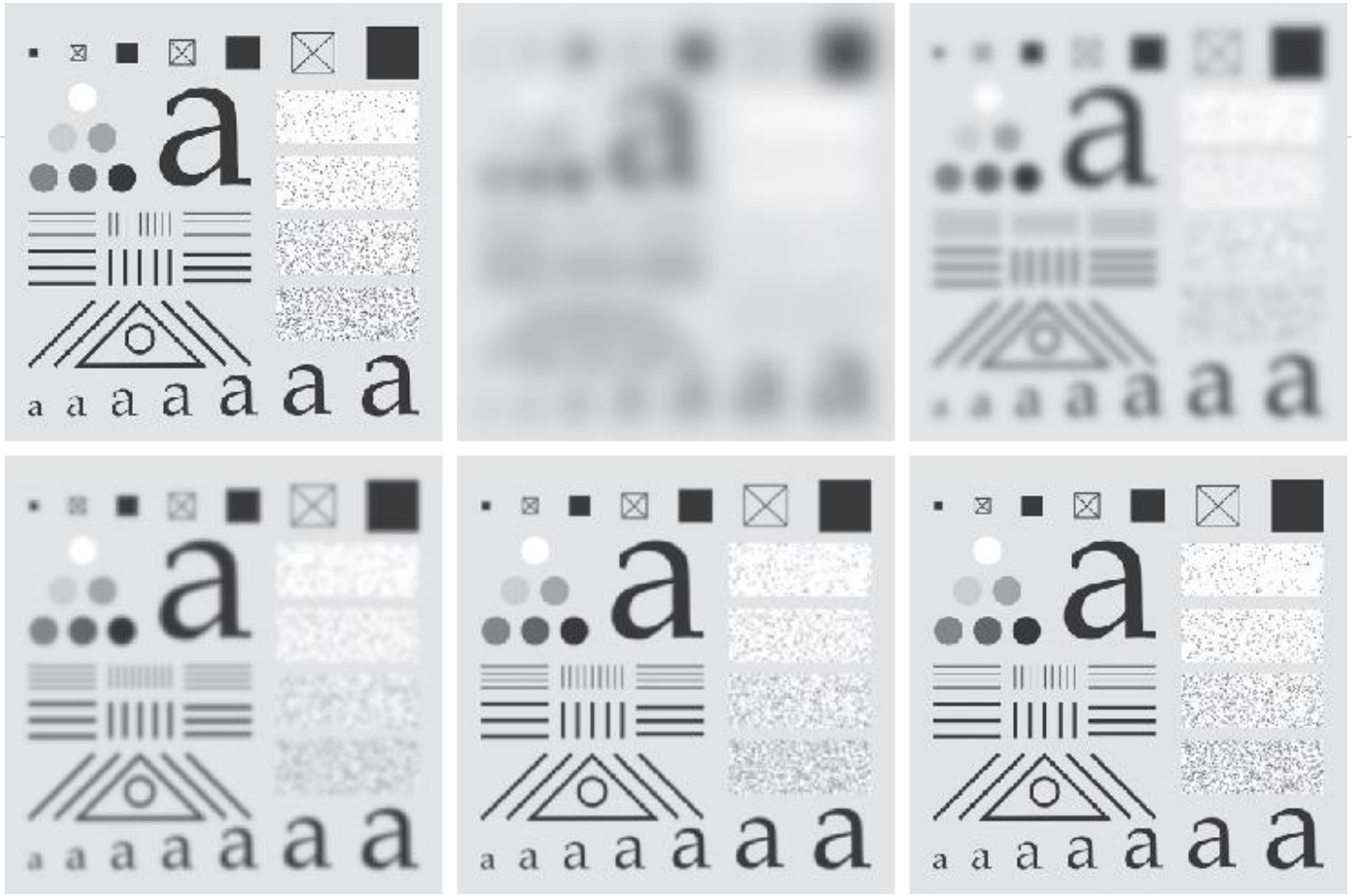

a b c
d e f

FIGURE 4.44 (a) Original image of size 688 × 688 pixels. (b)–(f) Results of filtering using GLPFs with cutoff frequencies at the radii shown in Fig. 4.40. Compare with Fig. 4.41. We used mirror padding to avoid the black borders characteristic of zero padding.

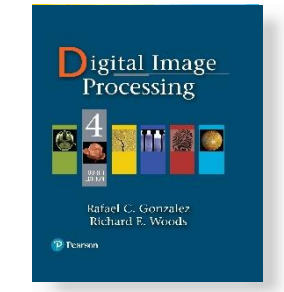

Chapter 4
Filtering in the Frequency Domain

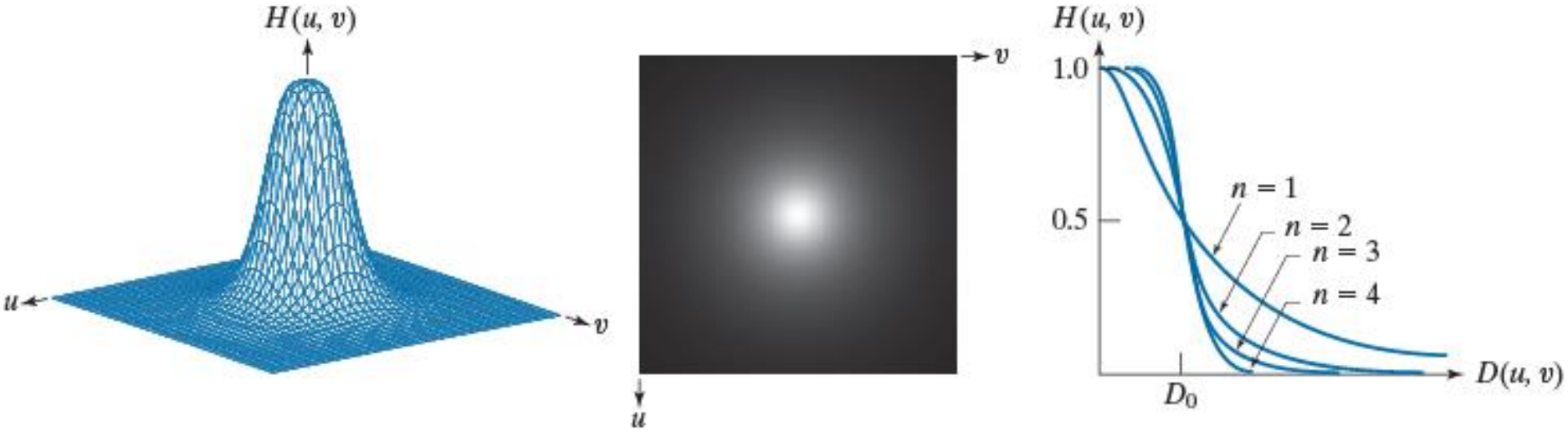

a b c

FIGURE 4.45 (a) Perspective plot of a Butterworth lowpass-filter transfer function. (b) Function displayed as an image. (c) Radial cross sections of BLPFs of orders 1 through 4.

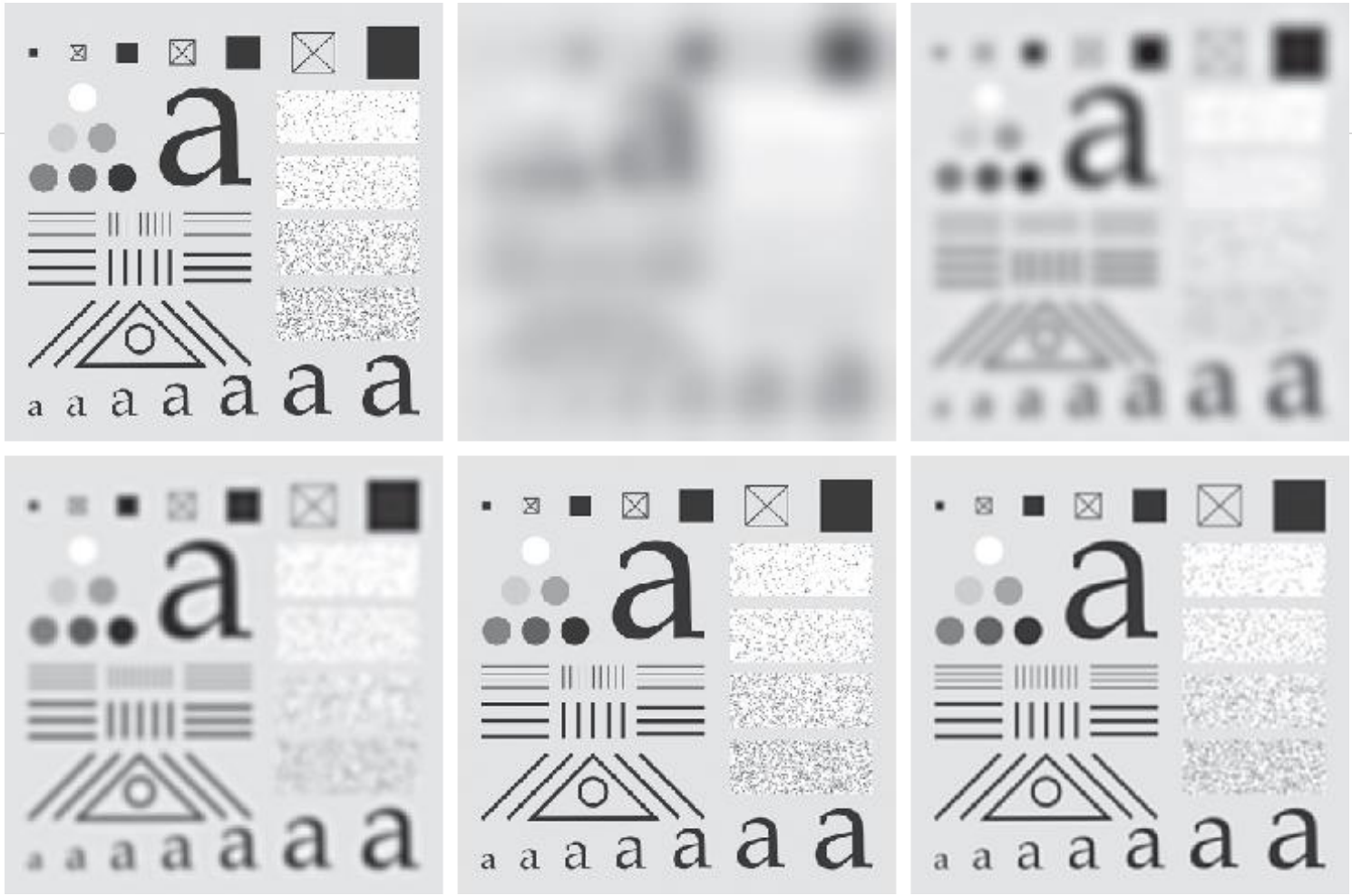

a b c
d e f

FIGURE 4.46 (a) Original image of size 688 × 688 pixels. (b)–(f) Results of filtering using BLPFs with cutoff frequencies at the radii shown in Fig. 4.40 and $n = 2.25$. Compare with Figs. 4.41 and 4.44. We used mirror padding to avoid the black borders characteristic of zero padding.

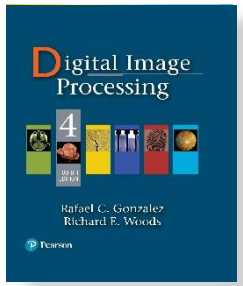

Chapter 4
Filtering in the Frequency Domain

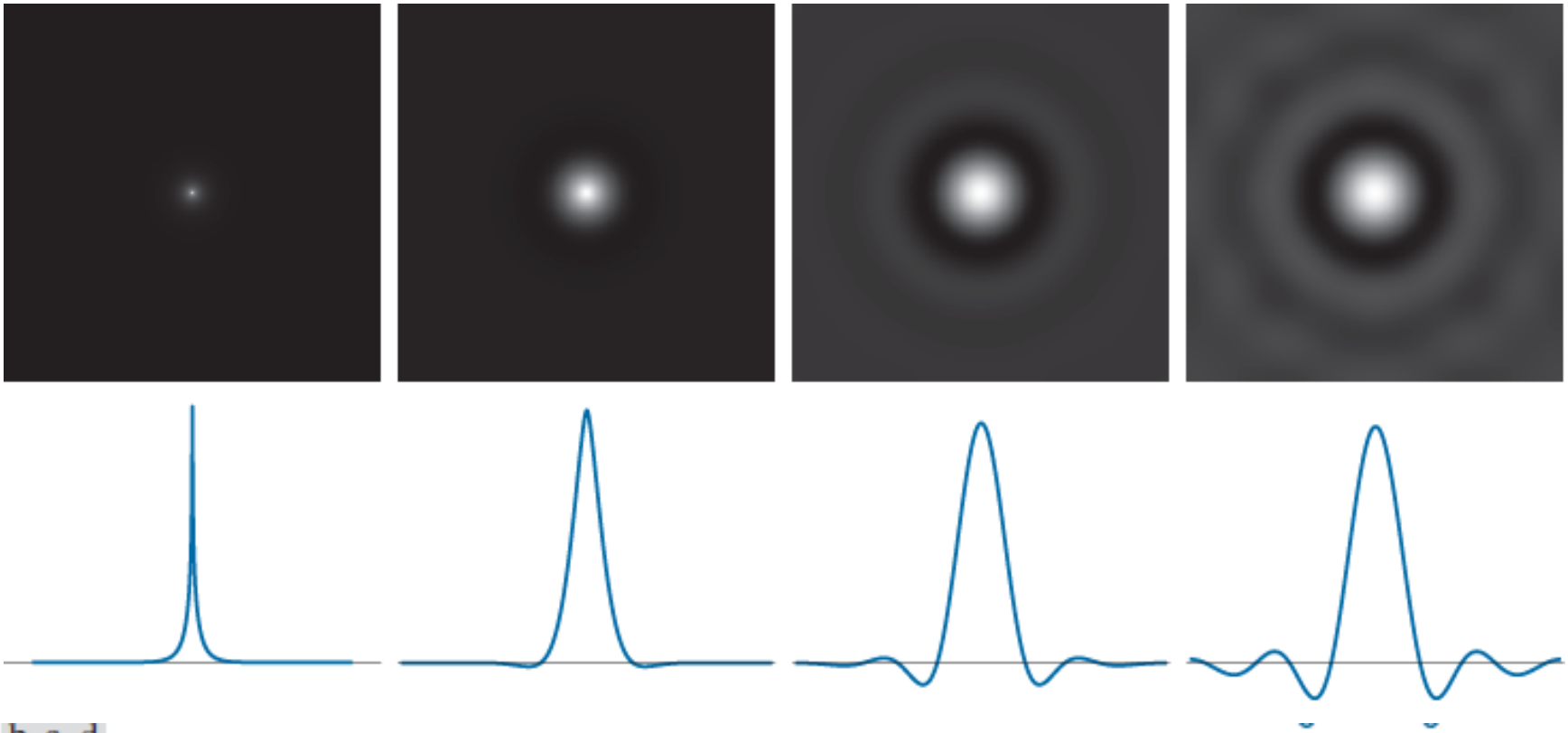

a b c d
e f g h

FIGURE 4.47 (a)–(d) Spatial representations (i.e., spatial kernels) corresponding to BLPF transfer functions of 1000 × 1000 pixels, cut-off frequency of 5, and order 1, 2, 5, and 20, respectively. (e)–(h) Corresponding inten profiles through the center of the filter functions.

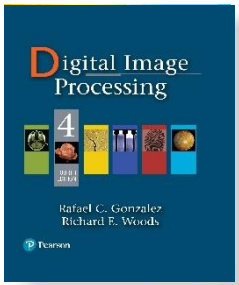

Chapter 4
Filtering in the Frequency Domain

TABLE 4.5
Lowpass filter transfer functions. D_0 is the cutoff frequency, and n is the order of the Butterworth filter.

Ideal	Gaussian	Butterworth
$H(u,v) = \begin{cases} 1 & \text{if } D(u,v) \le D_0 \\ 0 & \text{if } D(u,v) > D_0 \end{cases}$	$H(u,v) = e^{-D^2(u,v)/2D_0^2}$	$H(u,v) = \dfrac{1}{1 + \left[D(u,v)/D_0\right]^{2n}}$

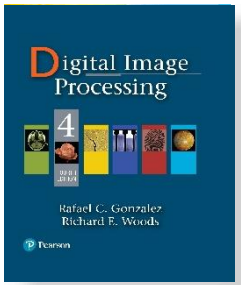

Chapter 4
Filtering in the Frequency Domain

a b

FIGURE 4.48
(a) Sample text of low resolution (note the broken characters in the magnified view). (b) Result of filtering with a GLPF, showing that gaps in the broken characters were joined.

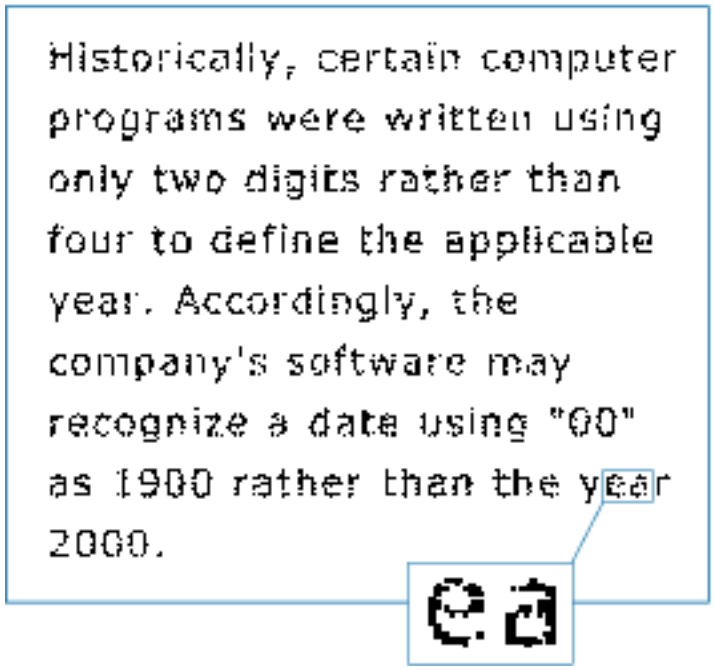

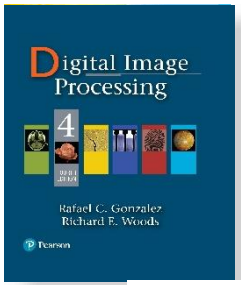

Chapter 4
Filtering in the Frequency Domain

a b c

FIGURE 4.49 (a) Original 785×732 image. (b) Result of filtering using a GLPF with $D_0 = 150$. (c) Result of filtering using a GLPF with $D_0 = 130$. Note the reduction in fine skin lines in the magnified sections in (b) and (c).

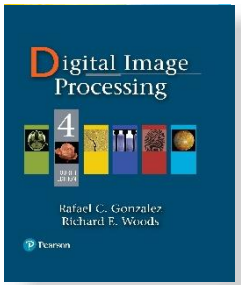

Digital Image Processing, 4th ed.

Gonzalez & Woods

www.ImageProcessingPlace.com

Chapter 4
Filtering in the Frequency Domain

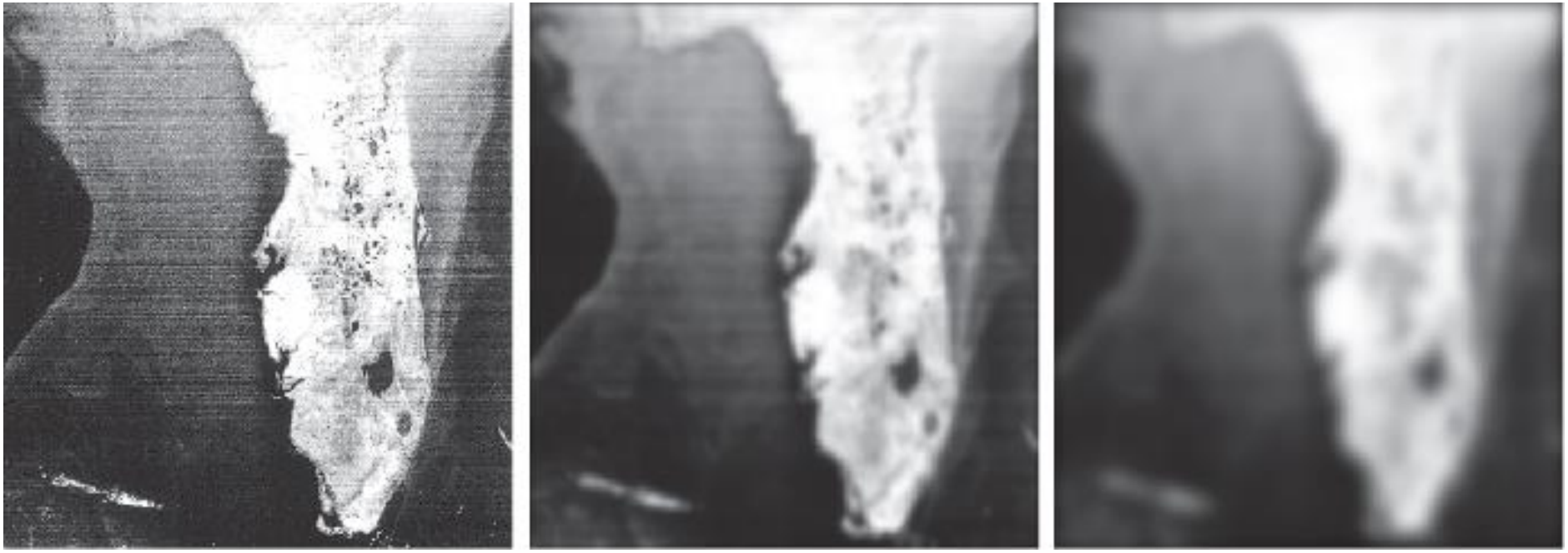

a b c

FIGURE 4.50 (a) 808 × 754 satellite image showing prominent horizontal scan lines. (b) Result of filtering using a GLPF with $D_0 = 50$. (c) Result of using a GLPF with $D_0 = 20$. (Original image courtesy of NOAA.)

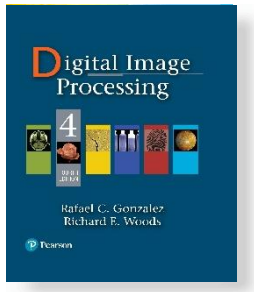

a b c
d e f
g h i

FIGURE 4.51 Top row: Perspective plot, image, and, radial cross section of an IHPF transfer function. Middle and bottom rows: The same sequence for GHPF and BHPF transfer functions. (The thin image borders were added for clarity. They are not part of the data.)

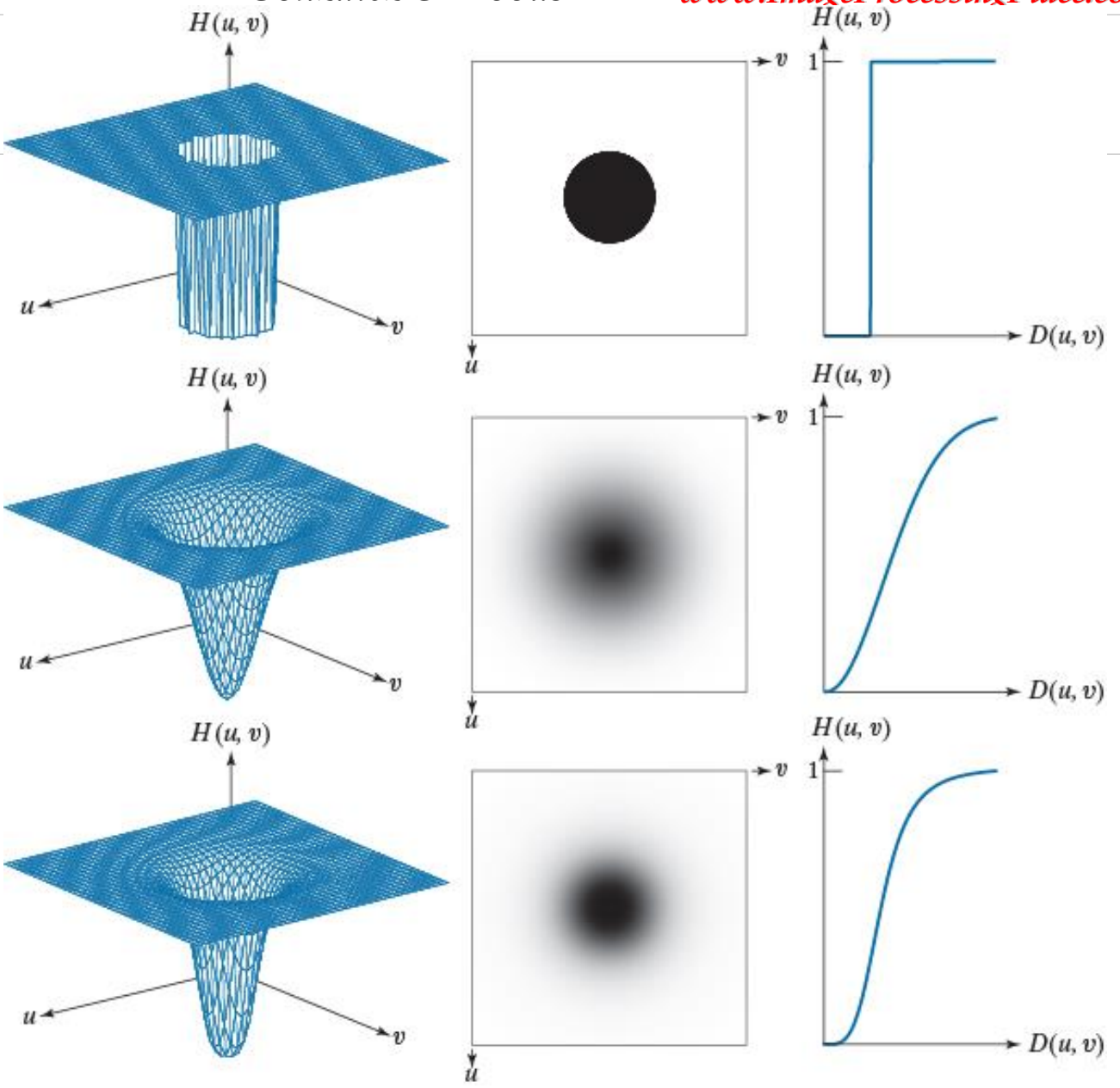

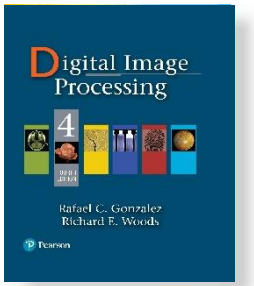

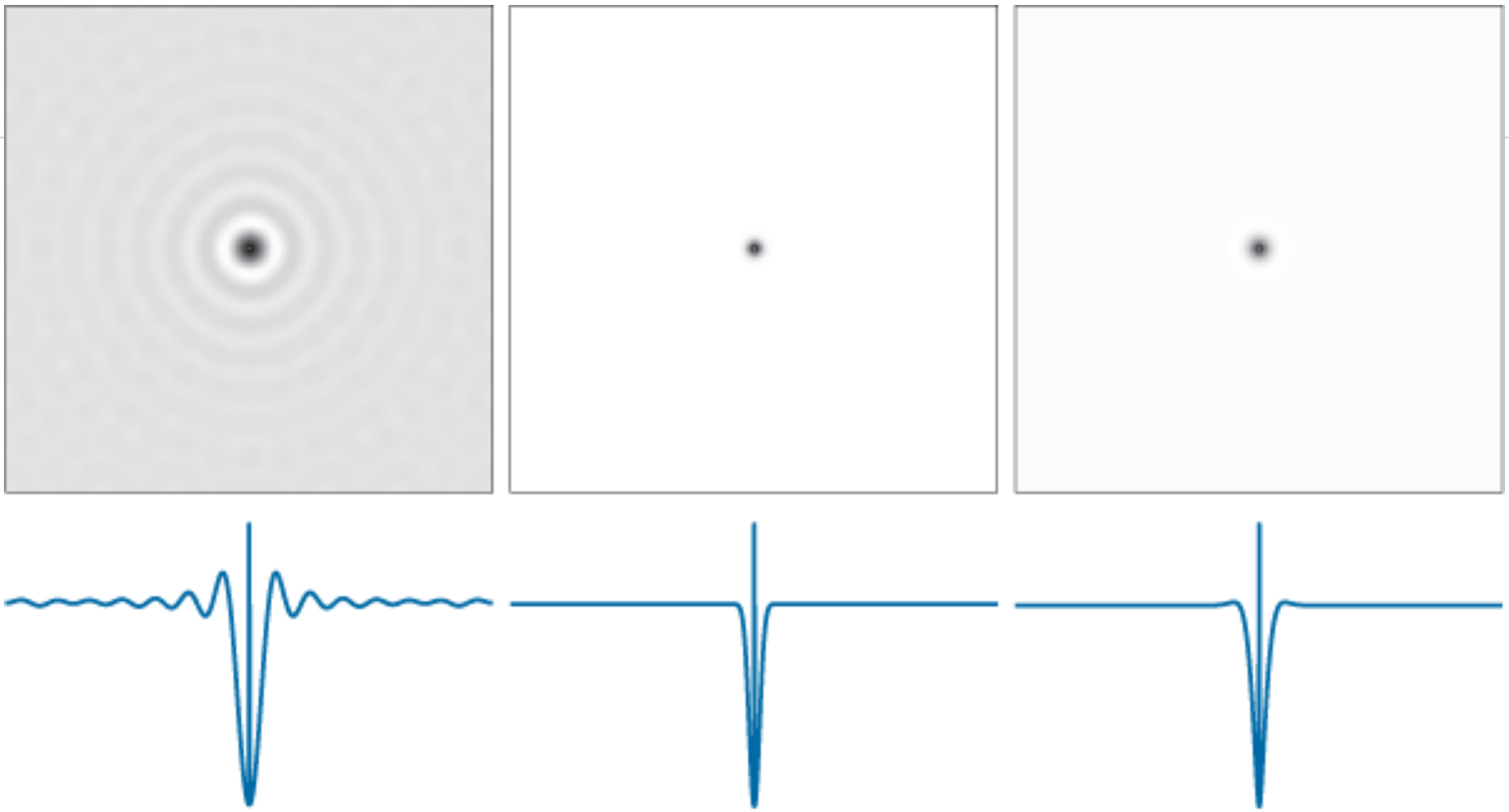

a b c
d e f

FIGURE 4.52 (a)–(c): Ideal, Gaussian, and Butterworth highpass spatial kernels obtained from IHPF, GHPF, and BHPF frequency-domain transfer functions. (The thin image borders are not part of the data.) (d)–(f): Horizontal intensity profiles through the centers of the kernels.

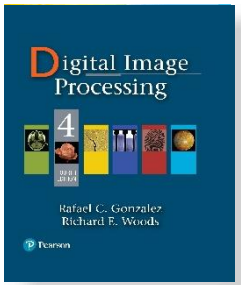

Chapter 4
Filtering in the Frequency Domain

TABLE 4.6
Highpass filter transfer functions. D_0 is the cutoff frequency and n is the order of the Butterworth transfer function.

Ideal	Gaussian	Butterworth
$H(u,v) = \begin{cases} 0 & \text{if } D(u,v) \le D_0 \\ 1 & \text{if } D(u,v) > D_0 \end{cases}$	$H(u,v) = 1 - e^{-D^2(u,v)/2D_0^2}$	$H(u,v) = \dfrac{1}{1 + \left[D_0/D(u,v)\right]^{2n}}$

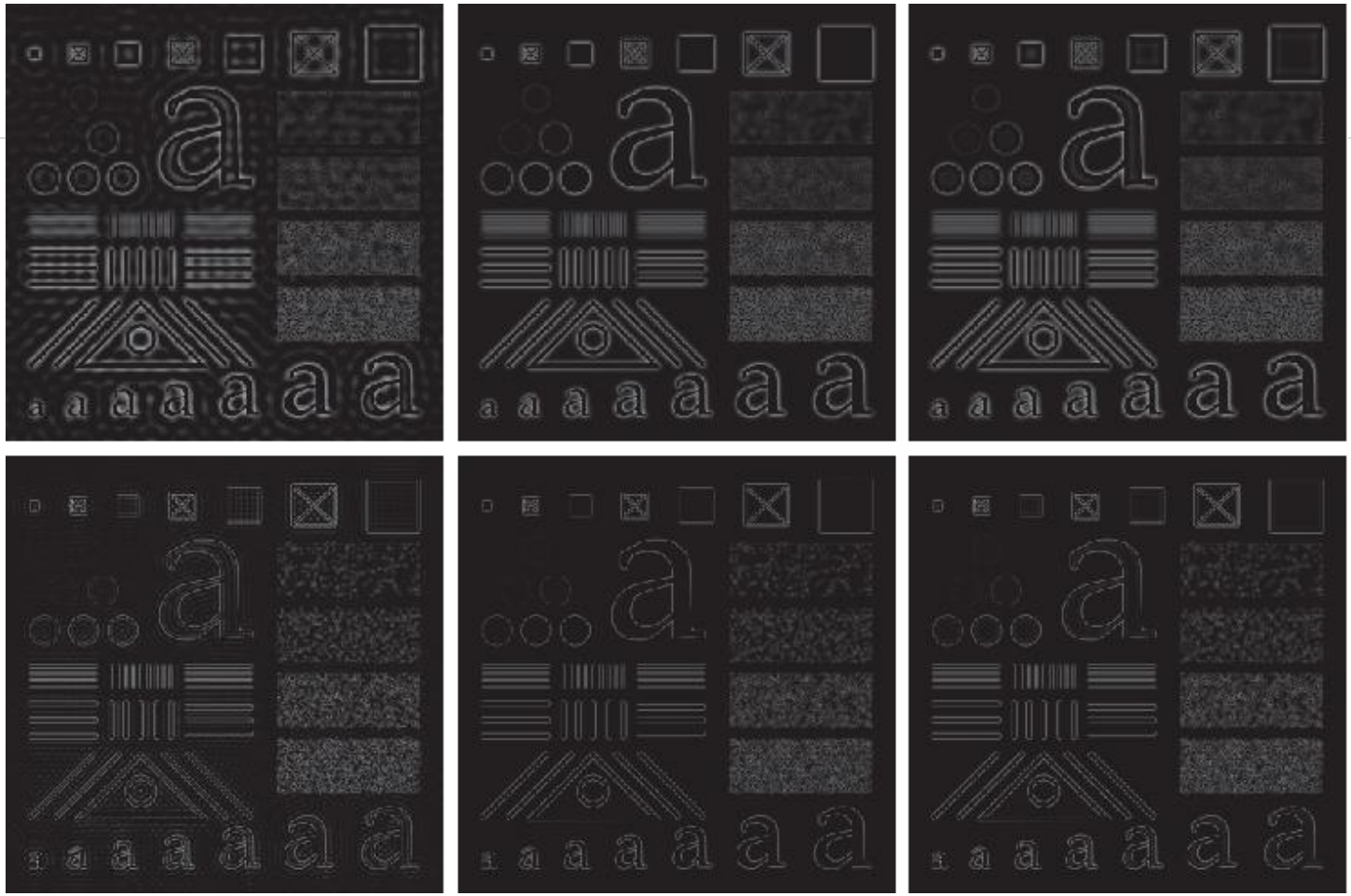

a b c
d e f

FIGURE 4.53 Top row: The image from Fig. 4.40(a) filtered with IHPF, GHPF, and BHPF transfer functions using $D_0 = 60$ in all cases ($n = 2$ for the BHPF). Second row: Same sequence, but using $D_0 = 160$.

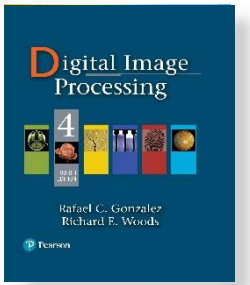

Chapter 4
Filtering in the Frequency Domain

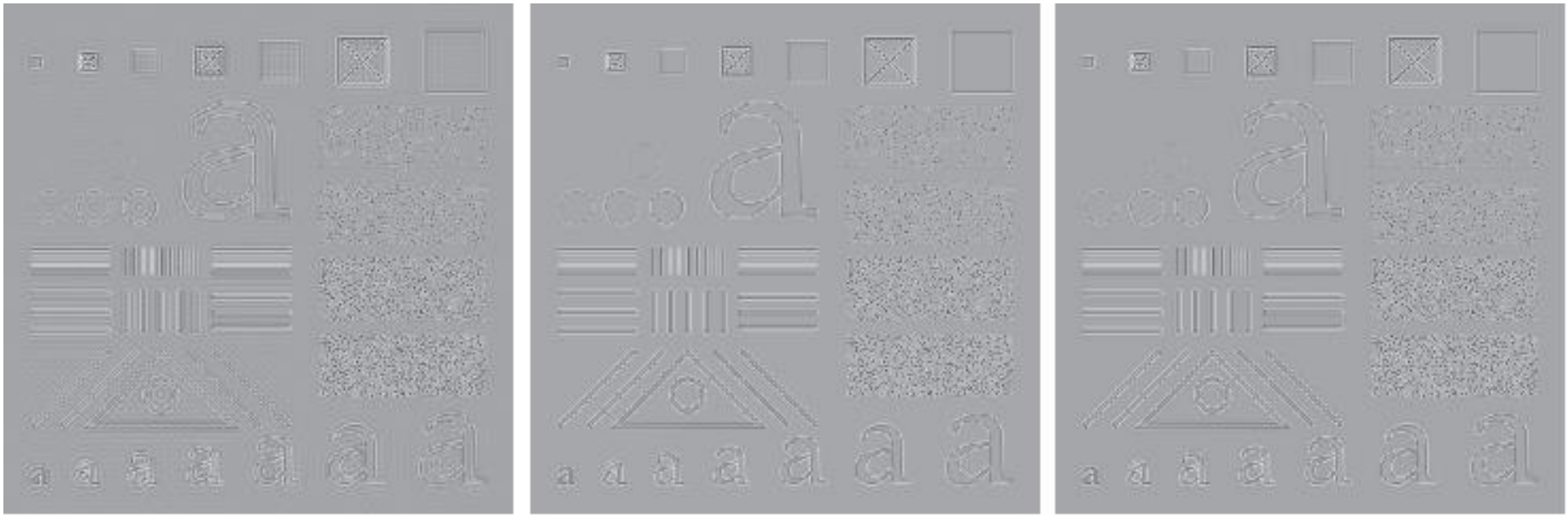

a b c

FIGURE 4.54 The images from the second row of Fig. 4.53 scaled using Eqs. (2-31) and (2-32) to show both positive and negative values.

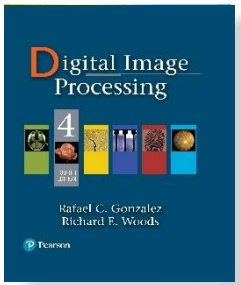

Digital Image Processing, 4th ed.

Gonzalez & Woods

www.ImageProcessingPlace.com

Chapter 4
Filtering in the Frequency Domain

a b c

FIGURE 4.55 (a) Smudged thumbprint. (b) Result of highpass filtering (a). (c) Result of thresholding (b). (Original image courtesy of the U.S. National Institute of Standards and Technology.)

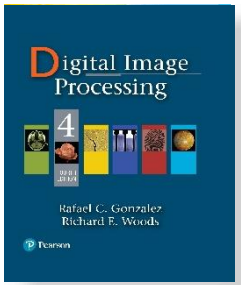

Chapter 4
Filtering in the Frequency Domain

a b

FIGURE 4.56
(a) Original, blurry image. (b) Image enhanced using the Laplacian in the frequency domain. Compare with Fig. 3.52(d). (Original image courtesy of NASA.)

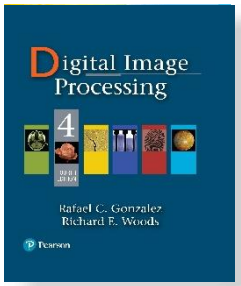

Chapter 4
Filtering in the Frequency Domain

a b
c d

FIGURE 4.57
(a) A chest X-ray. (b) Result of filtering with a GHPF function. (c) Result of high-frequency-emphasis filtering using the same GHPF. (d) Result of performing histogram equalization on (c). (Original image courtesy of Dr. Thomas R. Gest, Division of Anatomical Sciences, University of Michigan Medical School.)

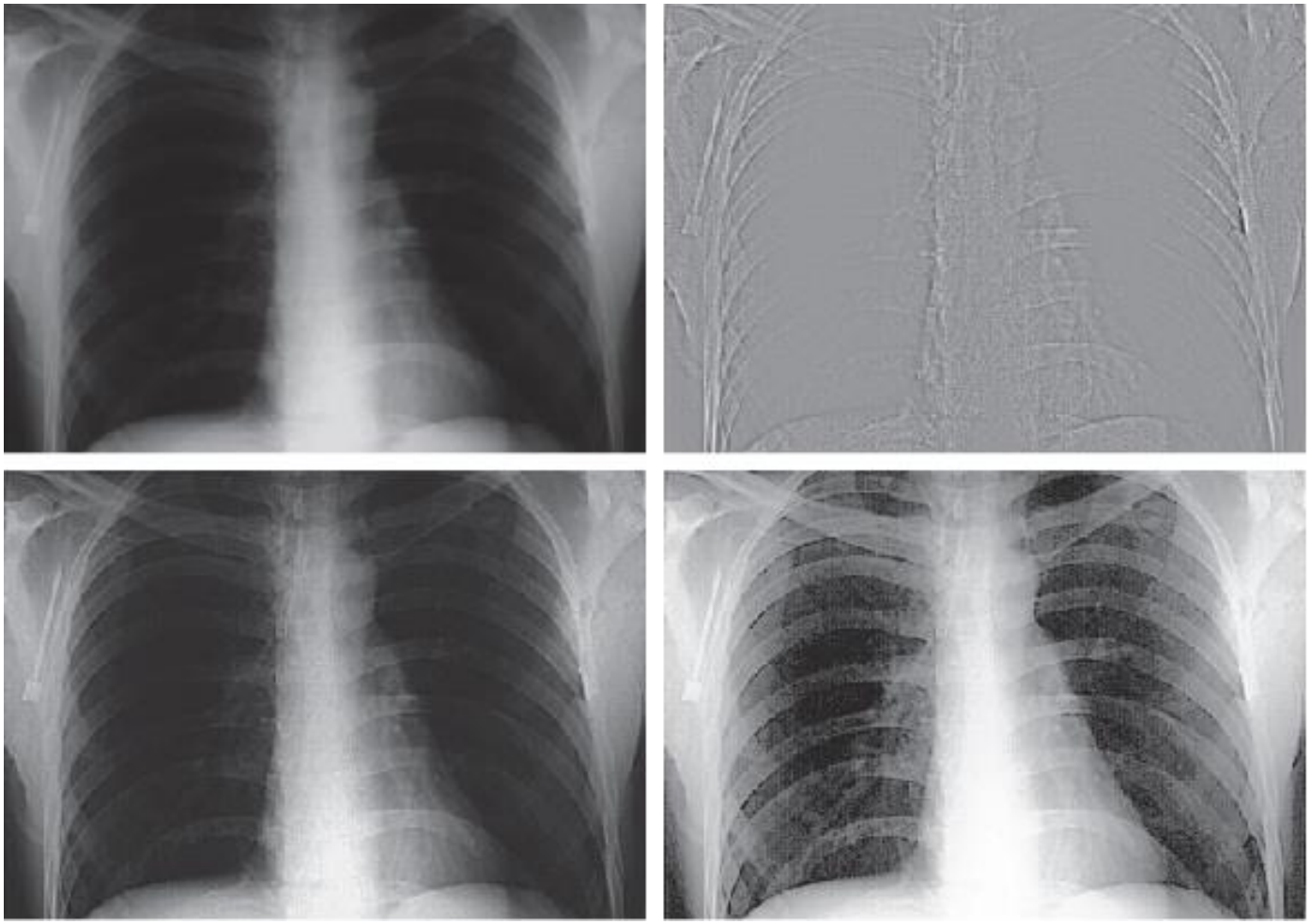

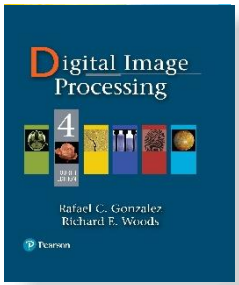

Chapter 4
Filtering in the Frequency Domain

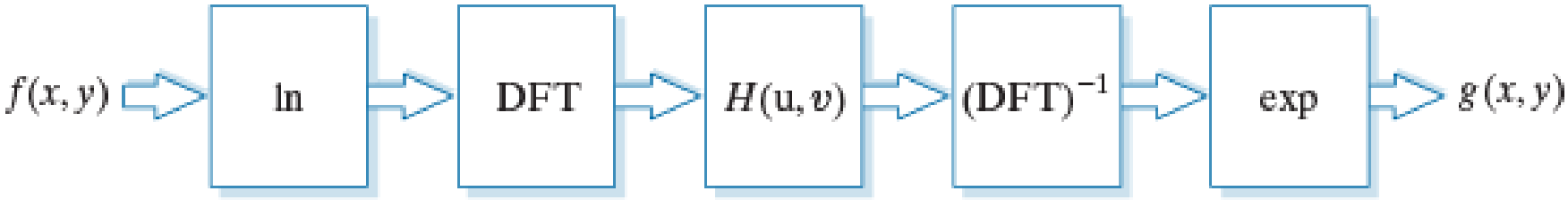

FIGURE 4.58
Summary of steps in homomorphic filtering.

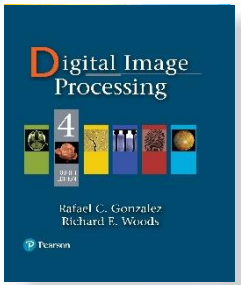

Chapter 4
Filtering in the Frequency Domain

FIGURE 4.59
Radial cross section of a homomorphic filter transfer function.

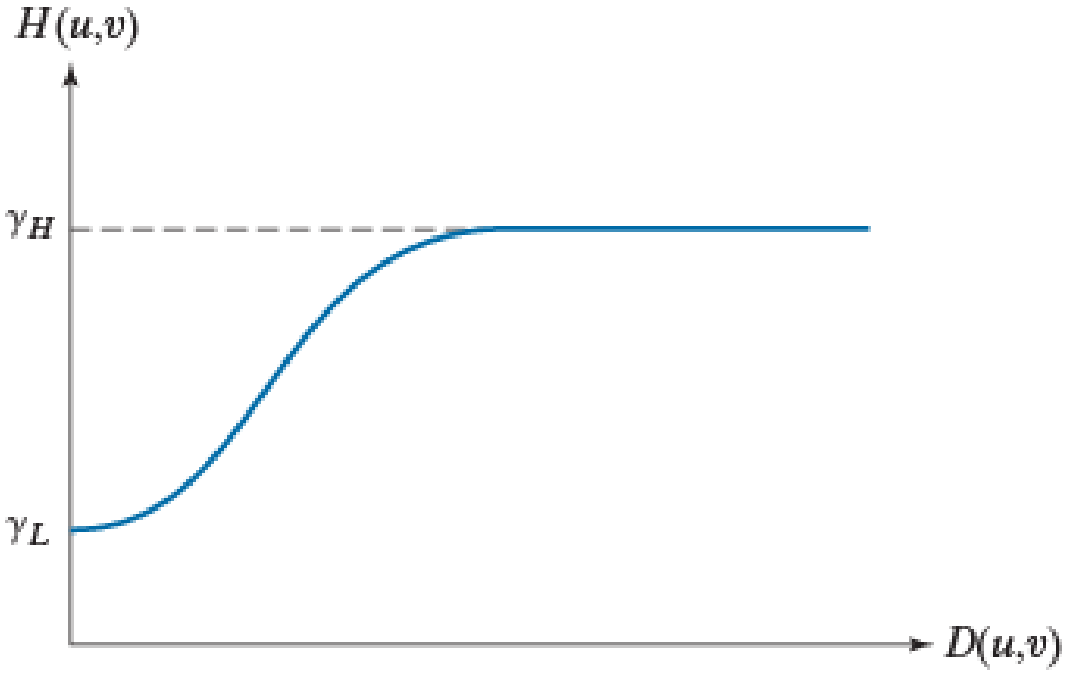

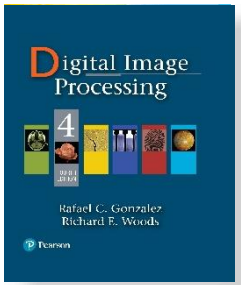

Chapter 4
Filtering in the Frequency Domain

a b

FIGURE 4.60
(a) Full body PET scan. (b) Image enhanced using homomorphic filtering. (Original image courtesy of Dr. Michael E. Casey, CTI Pet Systems.)

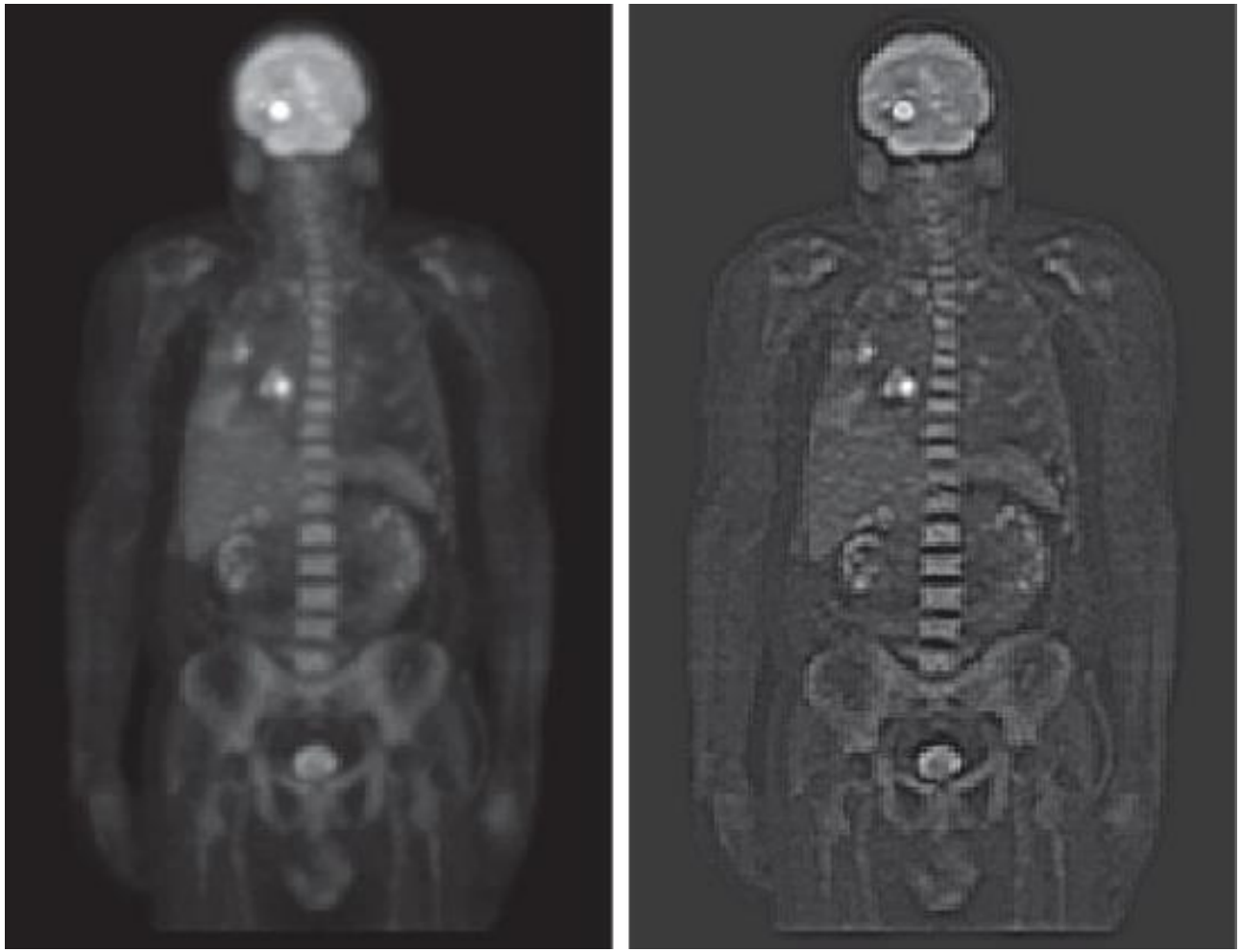

Chapter 4
Filtering in the Frequency Domain

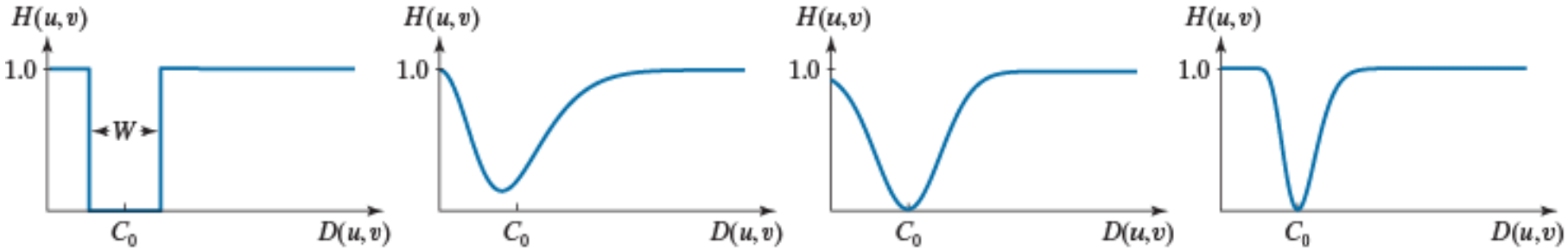

a b c d

FIGURE 4.61 Radial cross sections. (a) Ideal bandreject filter transfer function. (b) Bandreject transfer function formed by the sum of Gaussian lowpass and highpass filter functions. (The minimum is not 0 and does not align with C_0.) (c) Radial plot of Eq. (4-149). (The minimum is 0 and is properly aligned with C_0, but the value at the origin is not 1.) (d) Radial plot of Eq. (4-150); this Gaussian-shape plot meets all the requirements of a bandreject filter transfer function.

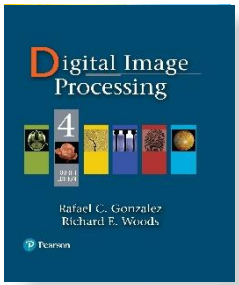

Chapter 4
Filtering in the Frequency Domain

TABLE 4.7
Bandreject filter transfer functions. C_0 is the center of the band, W is the width of the band, and $D(u,v)$ is the distance from the center of the transfer function to a point (u,v) in the frequency rectangle.

Ideal (IBRF)	Gaussian (GBRF)	Butterworth (BBRF)
$H(u,v) = \begin{cases} 0 & \text{if } C_0 - \frac{W}{2} \le D(u,v) \le C_0 + \frac{W}{2} \\ 1 & \text{otherwise} \end{cases}$	$H(u,v) = 1 - e^{-\left[\frac{D^2(u,v) - C_0^2}{D(u,v)W}\right]^2}$	$H(u,v) = \frac{1}{1 + \left[\frac{D(u,v)W}{D^2(u,v) - C_0^2}\right]^{2n}}$

Chapter 4
Filtering in the Frequency Domain

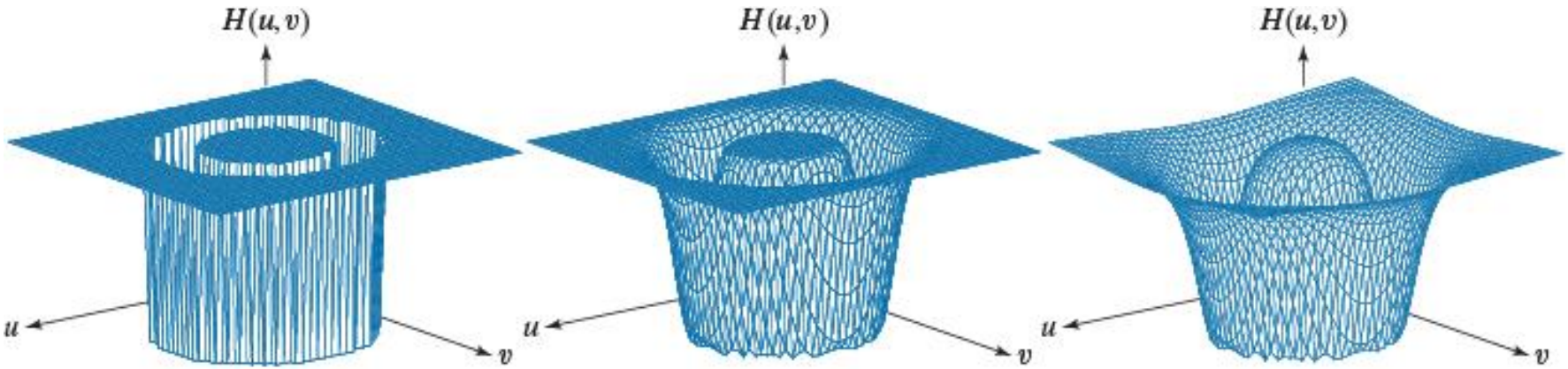

a b c

FIGURE 4.62 Perspective plots of (a) ideal, (b) modified Gaussian, and (c) modified Butterworth (of order 1) bandreject filter transfer functions from Table 4.7. All transfer functions are of size 512×512 elements, with $C_0 = 128$ and $W = 60$.

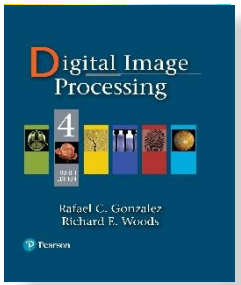

Chapter 4
Filtering in the Frequency Domain

a b c

FIGURE 4.63
(a) The ideal, (b) Gaussian, and (c) Butterworth bandpass transfer functions from Fig. 4.62, shown as images. (The thin border lines are not part of the image data.)

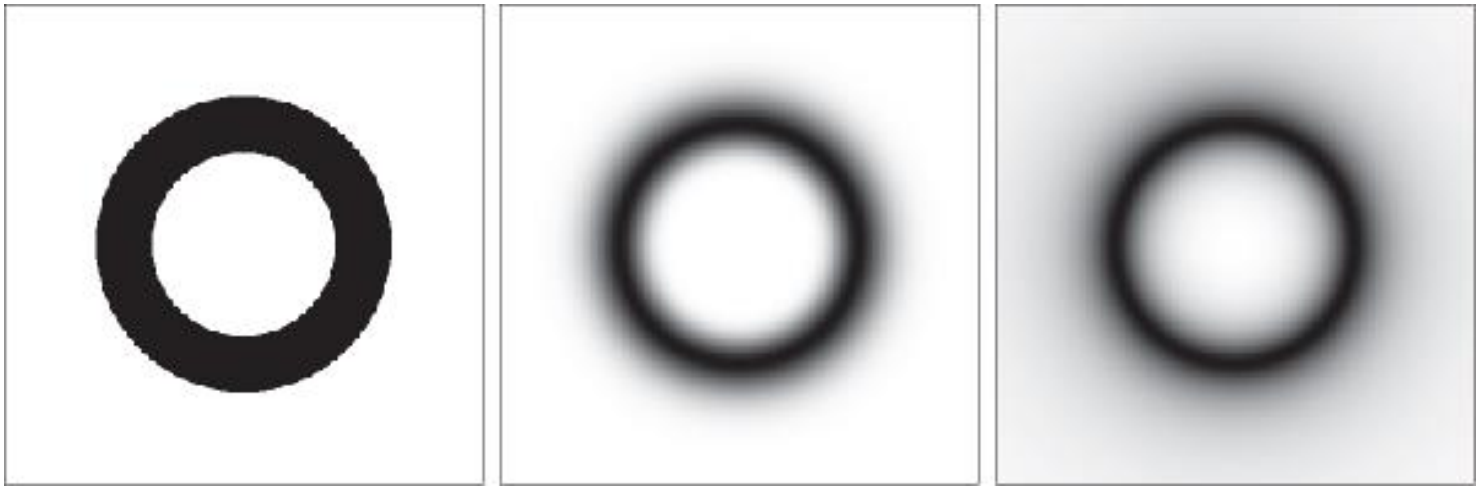

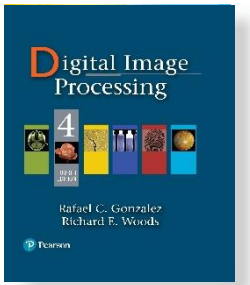

a b
c d

FIGURE 4.64
(a) Sampled newspaper image showing a moiré pattern. (b) Spectrum. (c) Fourier transform multiplied by a Butterworth notch reject filter transfer function. (d) Filtered image.

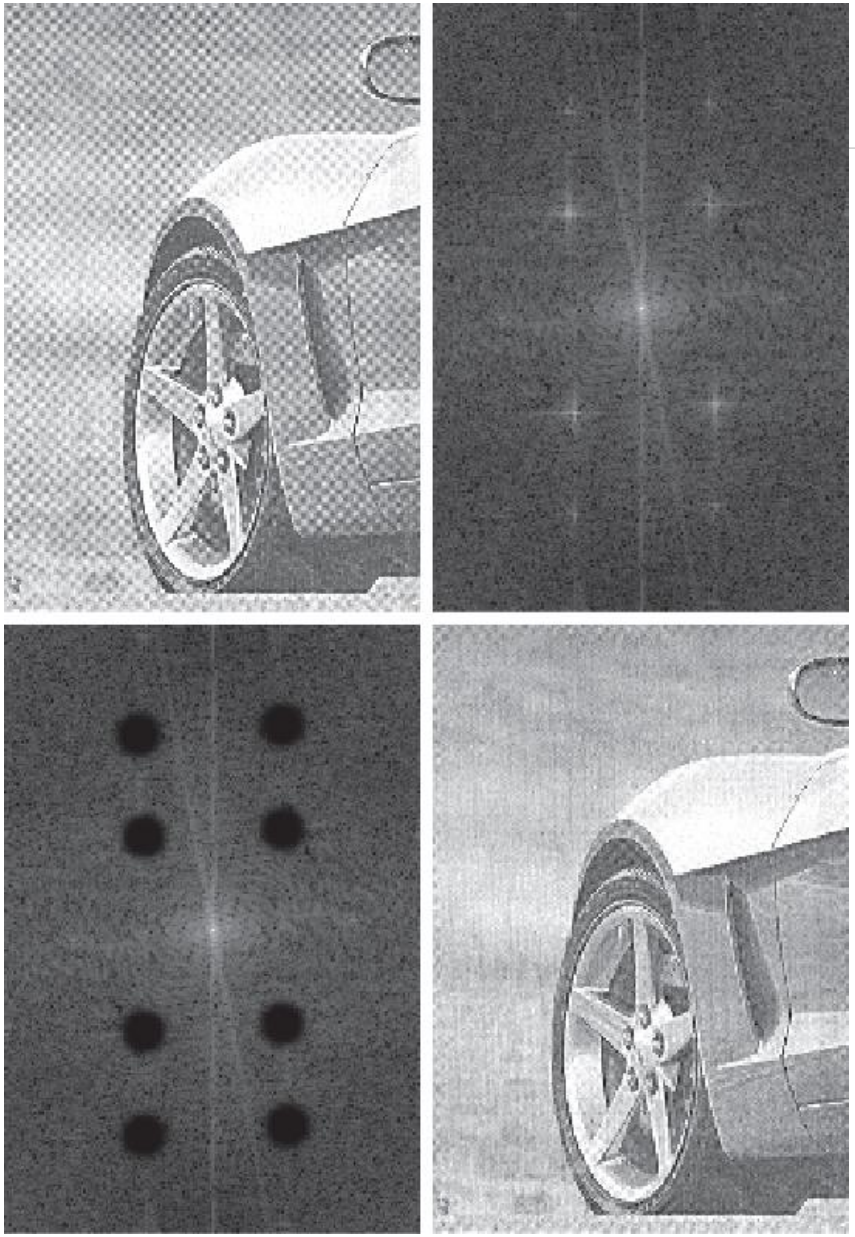

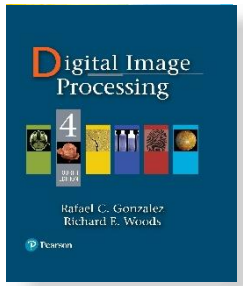

Chapter 4
Filtering in the Frequency Domain

a b
c d

FIGURE 4.65
(a) Image of Saturn rings showing nearly periodic interference. (b) Spectrum. (The bursts of energy in the vertical axis near the origin correspond to the interference pattern). (c) A vertical notch reject filter transfer function. (d) Result of filtering. (The thin black border in (c) is not part of the data.) (Original image courtesy of Dr. Robert A. West, NASA/ JPL.)

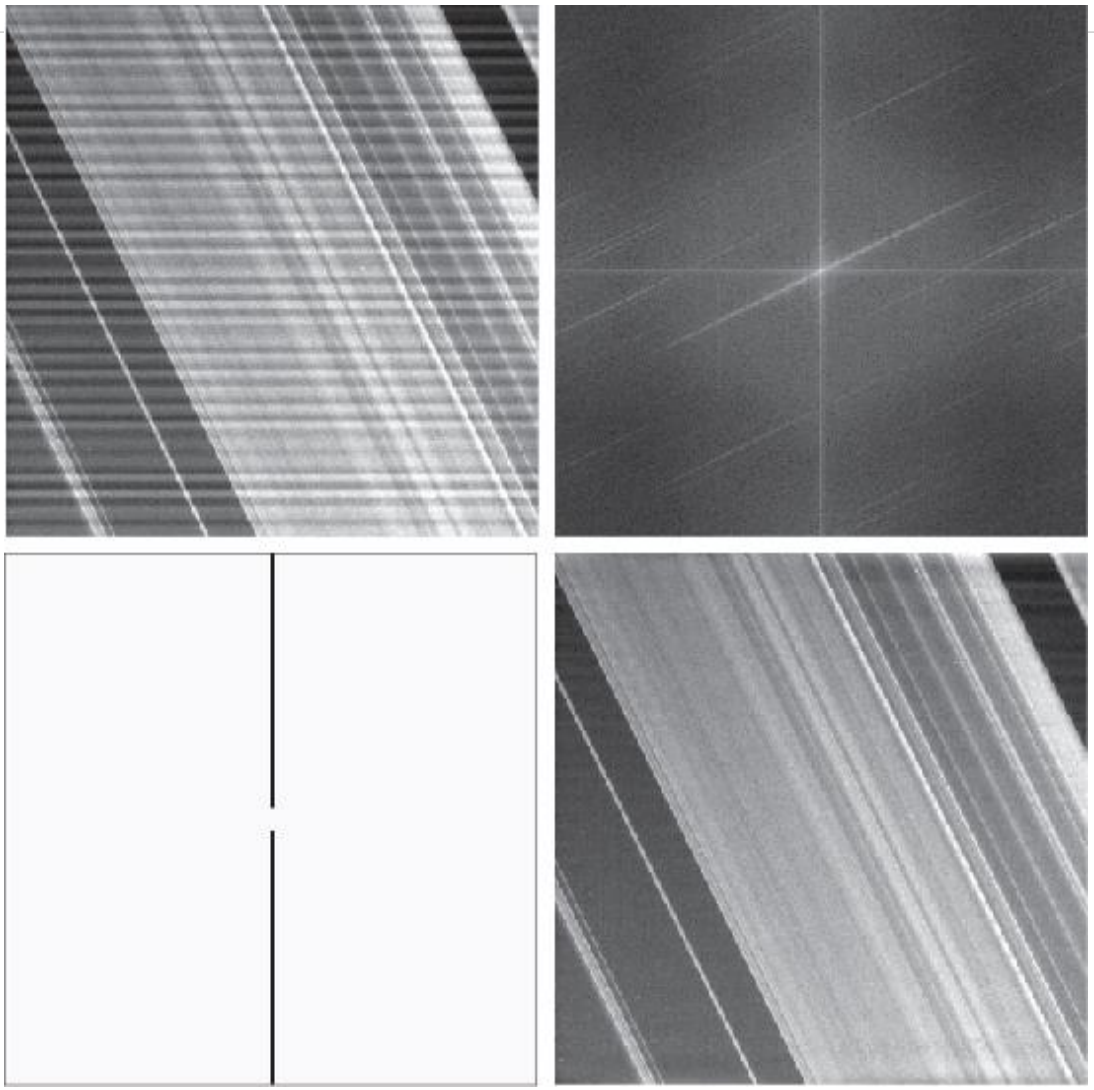

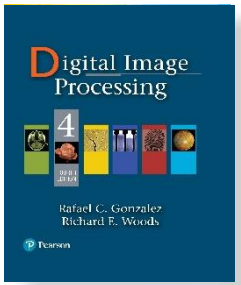

Chapter 4
Filtering in the Frequency Domain

a b

FIGURE 4.66
(a) Notch pass filter function used to isolate the vertical axis of the DFT of Fig. 4.65(a).
(b) Spatial pattern obtained by computing the IDFT of (a).

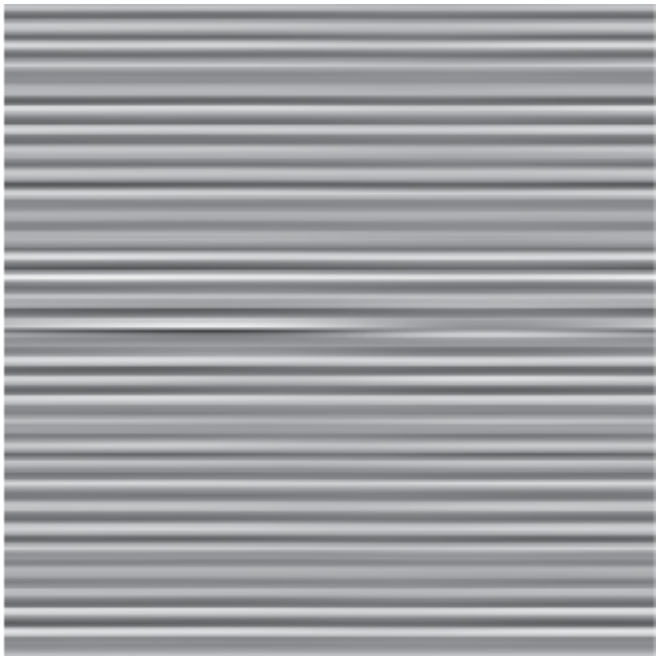

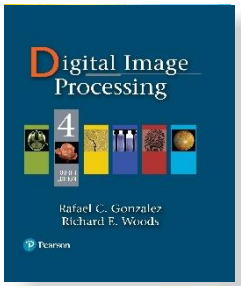

Chapter 4
Filtering in the Frequency Domain

FIGURE 4.67 Computational advantage of the FFT over a direct implementation of the 1-D DFT. The number of samples is $M = 2^p$. The computational advantage increases rapidly as a function of p.